

Lawrence Berkeley National Laboratory

LBL Publications

Title

Unraveling the functional dark matter through global metagenomics.

Permalink

<https://escholarship.org/uc/item/8700382s>

Journal

Nature, 622(7983)

Authors

Baltoumas, Fotis
Liu, Sirui
Selvitopi, Oguz
et al.

Publication Date

2023-10-01

DOI

10.1038/s41586-023-06583-7

Peer reviewed

Unraveling the functional dark matter through global metagenomics

<https://doi.org/10.1038/s41586-023-06583-7>

Received: 18 March 2022

Accepted: 30 August 2023

Published online: 11 October 2023

Open access

 Check for updates

Georgios A. Pavlopoulos^{1,2,3}✉, Fotis A. Baltoumas¹, Sirui Liu⁴, Oguz Selvitopi⁵, Antonio Pedro Camargo², Stephen Nayfach², Ariful Azad⁶, Simon Roux², Lee Call², Natalia N. Ivanova², I. Min Chen², David Paez-Espino², Evangelos Karatzas¹, Novel Metagenome Protein Families Consortium*, Ioannis Iliopoulos⁷, Konstantinos Konstantinidis⁸, James M. Tiedje⁹, Jennifer Pett-Ridge¹⁰, David Baker^{11,12,13}, Axel Visel², Christos A. Ouzounis^{2,14,15}, Sergey Ovchinnikov⁴, Aydin Buluç^{5,16} & Nikos C. Kyrpides²✉

Metagenomes encode an enormous diversity of proteins, reflecting a multiplicity of functions and activities^{1,2}. Exploration of this vast sequence space has been limited to a comparative analysis against reference microbial genomes and protein families derived from those genomes. Here, to examine the scale of yet untapped functional diversity beyond what is currently possible through the lens of reference genomes, we develop a computational approach to generate reference-free protein families from the sequence space in metagenomes. We analyse 26,931 metagenomes and identify 1.17 billion protein sequences longer than 35 amino acids with no similarity to any sequences from 102,491 reference genomes or the Pfam database³. Using massively parallel graph-based clustering, we group these proteins into 106,198 novel sequence clusters with more than 100 members, doubling the number of protein families obtained from the reference genomes clustered using the same approach. We annotate these families on the basis of their taxonomic, habitat, geographical and gene neighbourhood distributions and, where sufficient sequence diversity is available, predict protein three-dimensional models, revealing novel structures. Overall, our results uncover an enormously diverse functional space, highlighting the importance of further exploring the microbial functional dark matter.

Metagenome shotgun sequencing has become the method of choice for studying and classifying microorganisms from various biomes¹. With the latest advances in whole-genome sequencing technologies and the constant improvements in quality and cost efficiency, large-scale sequencing has become increasingly easier, faster and more affordable. This has led to a considerable increase in metagenomic sequencing data over the past few years, therefore making them an indispensable resource for investigating the microbial dark matter².

To elucidate the genetic composition of a metagenomic sample, two major approaches are typically used, each with distinct advantages and disadvantages. In the first, sequencing reads are accurately mapped to a known, annotated set of reference genome sequences to provide a quick overview of the presence of known organisms, genes and potential functions. MG-RAST⁴ is one system that excels in this type of analysis. In the second approach, massive de novo assembly of the reads into

contigs/scaffolds can provide invaluable insights into the presence of previously undescribed organisms and their genetic makeup. Recent technological advancements in assembly and binning tools⁵ have led to a significant increase in the assembled fraction of the average metagenome, coupled with a parallel exponential increase in the number of metagenome-assembled genomes (MAGs). Data management and comparative analysis systems supporting this type of data include Integrated Microbial Genomes & Microbiomes (IMG/M)⁶ and MGnify⁷.

However, both approaches share the same major limitation with respect to gene functional annotation, which relies on predicting function by homology searching against reference protein databases, such as COG⁸, Pfam³ and KEGG Orthology⁹. As a result, any genes predicted in assembled metagenomic data that do not map to reference protein families are typically ignored and dropped from subsequent comparative analysis. To eliminate this reliance on reference datasets and to

¹Institute for Fundamental Biomedical Research, Biomedical Science Research Center Alexander Fleming, Vari, Greece. ²DOE Joint Genome Institute, Lawrence Berkeley National Laboratory, Berkeley, CA, USA. ³Center for New Biotechnologies and Precision Medicine, School of Medicine, National and Kapodistrian University of Athens, Athens, Greece. ⁴John Harvard Distinguished Science Fellowship Program, Harvard University, Cambridge, MA, USA. ⁵Computational Research Division, Lawrence Berkeley National Laboratory, Berkeley, CA, USA. ⁶Luddy School of Informatics, Computing and Engineering, Indiana University Bloomington, Bloomington, IN, USA. ⁷Department of Basic Sciences, School of Medicine, University of Crete, Heraklion, Greece. ⁸School of Civil and Environmental Engineering, Georgia Institute of Technology, Atlanta, GA, USA. ⁹Center for Microbial Ecology, Michigan State University, East Lansing, MI, USA. ¹⁰Physical and Life Sciences Directorate, Lawrence Livermore National Laboratory, Livermore, CA, USA. ¹¹Department of Biochemistry, University of Washington, Seattle, WA, USA. ¹²Institute for Protein Design, University of Washington, Seattle, WA, USA. ¹³Howard Hughes Medical Institute, University of Washington, Seattle, WA, USA. ¹⁴Biological Computation & Process Laboratory, Chemical Process & Energy Resources Institute, Centre for Research & Technology Hellas, Thessalonica, Greece. ¹⁵Biological Computation & Computational Biology Group, Artificial Intelligence & Information Analysis Lab, School of Informatics, Aristotle University of Thessalonica, Thessalonica, Greece. ¹⁶Department of Electrical Engineering and Computer Sciences, University of California, Berkeley, CA, USA. *A list of authors and their affiliations appears at the end of the paper. ✉e-mail: pavlopoulos@fleming.gr; nckyrpides@lbl.gov

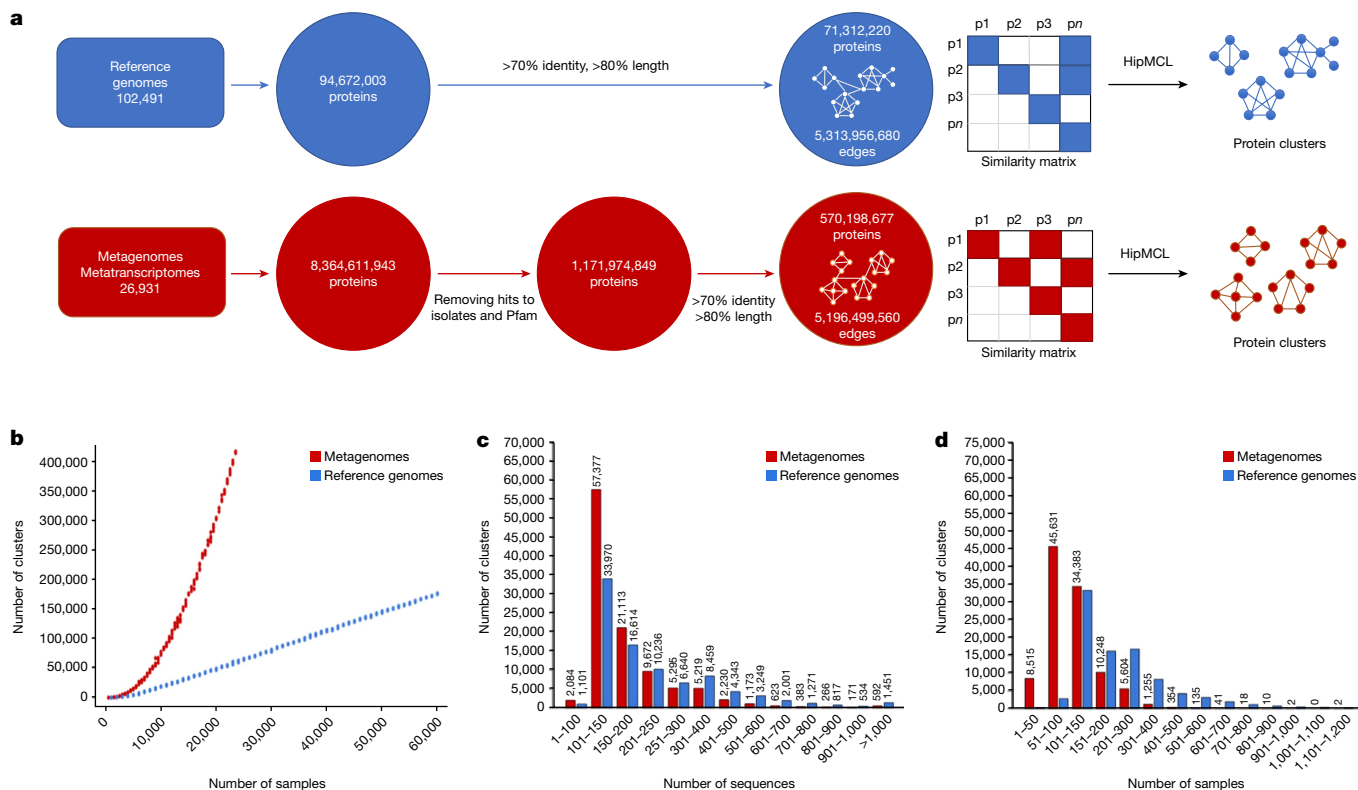


Fig. 1 | Sequence clustering overview. **a**, Clustering proteins from the reference genome (blue) and ED (red) datasets. **b**, Rarefaction curves of protein clusters for reference genome (blue) and ED (red) datasets. **c,d**, Bar chart

visualization and comparison of cluster components per cluster for the number of sequences (**c**) and the number of genome or ED samples (**d**).

estimate the breadth of unexplored functional diversity, referred to as the functional dark matter, an all-versus-all metagenomic comparison is required. Such a task requires considerable computational resources, yet reaching such levels of scalability remains technically challenging. Although some excellent efforts to address this issue have been recently reported^{10–12}, metagenomes have not yet been comprehensively surveyed to uncover the functional dark matter.

Here we present a scalable computational approach for identifying and characterizing functional dark matter found in metagenomes. First, we identified the novel protein space present in 26,931 metagenomic datasets from IMG/M, after removing all genes with matches to the IMG database of over 100,000 reference genomes or Pfam. We next clustered the remaining sequences into protein families and explored their taxonomic and biome distributions and, where possible, predicted their tertiary (three-dimensional (3D)) structures.

The novel protein sequence space

We initially collected all protein sequences (longer than 35 amino acid residues) from all public reference genomes and assembled metagenomes and metatranscriptomes hosted in the IMG/M platform⁶. In total, we extracted all protein sequences from 89,412 bacterial, 9,202 viral, 3,073 archaeal and 804 eukaryal genomes, resulting in a final dataset of 94,672,003 sequences. The reference genomes included in this study consisted solely of isolate genomes, not MAGs or single-amplified genomes. Similarly, for unbinned metagenomes, we extracted all predicted protein sequences from scaffolds of at least 500 bp and with lengths of at least 35 amino acids from 26,931 datasets (20,759 metagenomes and 6,172 metatranscriptomes), hereafter referred to as the environmental dataset (ED). This resulted in a non-redundant set of 8,364,611,943 predicted proteins or protein fragments. To identify the functional dark-matter component of this dataset, we first discarded

any protein sequence with hits to Pfam⁸ or to any sequences from the reference genome set. The final non-redundant catalogue representing the unexplored metagenomic protein space consisted of 1,171,974,849 protein sequences (14% of the total).

Novel protein families

We next clustered the 1.1 billion ED proteins using a graph-based approach. For comparative purposes, we followed the same approach for the 94 million proteins from reference genomes. First, an all-versus-all similarity matrix was built for each of the two gene catalogues (that is, proteins from reference genomes and those from the ED) by calculating all significant pairwise sequence similarities. Each of the two graphs was then analysed to identify sequence-similarity-based protein clusters. For this purpose, we used HipMCL¹³, a massively parallel implementation of the original MCL algorithm¹⁴ that was previously developed for this scale of data and that can run on distributed-memory computers. The whole process from data retrieval to cluster generation is shown in Fig. 1a.

Although most clusters with at least 50 members (and possibly even those with at least 25 members) probably represent potentially functionally important clusters, we restricted the subsequent analysis to the larger families with at least 100 members to focus on higher-quality data as well as better candidates for predicting structures (Table 1). In total, we identified 106,198 families with at least 100 members that will be referred to as novel metagenome protein families (NMPFs) (Table 1 (right column)). For comparison, we identified 92,909 protein clusters in the corresponding set of protein clusters with at least 100 members from reference genomes. By directly comparing the two clustered sets (reference versus ED protein clusters), we observed an increase in the ED protein clusters by greater than 14-fold for clusters with at least 3 members, greater than 3-fold for clusters with at least 25 members,

Table 1 | HipMCL clustering of proteins from reference genomes and metagenomes and their corresponding clusters of different protein family sizes (cumulative)

Environmental dataset					
Proteins for clustering	570,198,677				
Cluster size	≥3 members	≥25 members	≥50 members	≥75 members	≥100 members
Clusters (NMPFs)	64,149,288	1,501,861	428,910	200,075	106,198
Datasets	24,477	23,208	21,447	20,274	19,326
Scaffolds	349,547,957	71,910,494	39,593,021	27,041,114	17,280,119
Proteins	400,241,252	77,892,505	42,280,078	28,621,670	19,986,348
Percentage of proteins	70.19	13.66	7.41	5.02	3.5
Reference genomes					
Proteins for clustering	71,312,320				
Cluster size	≥3 members	≥25 members	≥50 members	≥75 members	≥100 members
Clusters	4,572,038	415,591	197,965	128,324	92,909
Datasets	80,896	77,611	76,294	75,145	74,134
Proteins	64,427,269	38,509,539	31,100,303	26,906,094	23,860,313
Percentage of proteins	90.34	54.00	43.61	37.73	33.46

around a 2-fold increase for clusters with at least 50 and 75 members as well as an increase for clusters with at least 100 members (Table 1). Although the metagenome sequence space is intrinsically more fragmented compared with the reference genomes (Supplementary Methods and Supplementary Fig. 1), and a higher percentage of genes would be erroneous or incomplete (which is also one of the reasons we decided to focus all further analysis on the larger clusters), these results also suggest that much of protein sequence space remains to be explored. This is also supported by rarefaction curves generated from the ≥100-member clusters (Fig. 1b). These curves show that, as more samples become available, the cluster number increases linearly for reference genomes but exponentially, without reaching a plateau, for metagenomes.

Biome distribution

To determine the biome distribution landscape of the NMPFs, the corresponding metadata were collected for each sample from IMG/M⁶ using the GOLD database¹⁵ ecosystem classification scheme¹⁶ (Supplementary Table 1). The biome distribution of the NMPFs is shown in Fig. 2a,b and Extended Data Fig. 1. Here the three main GOLD ecosystems (environmental, host-associated and engineered) are further divided into eight more specific ecosystem types: freshwater, marine, soil, plants, human, non-human mammals, other host-associated and engineered. Examining the network topology, we observed minimum gene sharing within each NMPF across the three broad ecosystems, in accordance with recent observations of protein families from 13,174 metagenomes¹⁷, with the exception of soil/plant associations (see below). However, 7,692 NMPFs (7%) were found to have members across all of the eight ecosystem types. The properties of the top NMPFs distributed across all ecosystem types are shown in Supplementary Table 2, while the properties of the top NMPFs of each distinct ecosystem type are shown in Supplementary Tables 3 and 4. In addition to the analysis presented above, each ecosystem was further divided into subcategories for finer analysis (Extended Data Figs. 2–5 and Supplementary Fig. 2).

The largest number of NMPFs was shared between soil and plant environments (62% of the soil and 96% of plant-associated families), as would be expected due to the strong overlap of the sampling in these ecosystems (that is, most of the plant samples are from the rhizosphere) (Fig. 2a and Extended Data Fig. 3). This was followed by NMPFs shared between soil and freshwater, which could be primarily due to the assignment of wetland and sediment samples under the freshwater ecosystem

classification. For the same reason, we observed a notable overlap between plants and freshwater NMPFs as well as between soil, freshwater and plant NMPFs. Conversely, only 37% of freshwater and 46% of marine NMPFs were shared with each other. Even fewer protein families were shared between ecosystem types such as human, non-human mammals and host-associated. On the other hand, a rather substantial overlap in NMPFs between human and engineered environments was observed (Fig. 2). This is not surprising, considering that engineered environments largely contain samples from human-waste-related ecosystems (such as solid waste and wastewater). Similarly, an overlap exists between freshwater and engineered environments, as well as between freshwater and host-associated types (human, non-human mammals and other host-associated), as shown in Extended Data Fig. 1. These overlaps could be indicative of phenomena such as faecal contamination of freshwater environments, leading to the co-occurrence of the same NMPFs—and, therefore, the same microbial communities—in different ecosystem types.

The percentage of ecosystem-specific NMPFs varied significantly across each of the eight ecosystem types, with the highest percentage observed for host-associated (non-human mammals) (85.6%) and host-associated (other) samples (79.2%), followed by marine (48.4%) and then soil (14.2%) samples (Fig. 2c). This is explained by the unique characteristics of the environments contained in these ecosystem categories, for example, oceanic environments of marine samples, and even more so in the case of the host-associated category, which contains a diverse array of microbiome hosts with significant biological differences (for example, arthropods and annelids) (Extended Data Fig. 4). In contrast to marine samples, freshwater samples had a very small percentage of ecosystem-type-specific families, mostly due to a large number of wetland and sediment samples with strong associations with soil, as did the plant/rhizosphere-related samples with soil samples (Fig. 2a).

Finally, to investigate the ecosystem distribution of NMPFs, the ecosystem prevalence of the most-abundant NMPFs of each ecosystem type was evaluated. The prevalence of each NMPF in an ecosystem (for example, freshwater) was calculated as the number of family ecosystem-associated datasets over the total number of ecosystem-associated datasets in the study (Supplementary Table 3). Despite the existence of NMPFs strongly associated with a particular ecosystem type (for example, >80% of NMPFs), their prevalence in the overall datasets associated with said ecosystems was rather low, with most NMPFs distributed across 5–20% of the samples

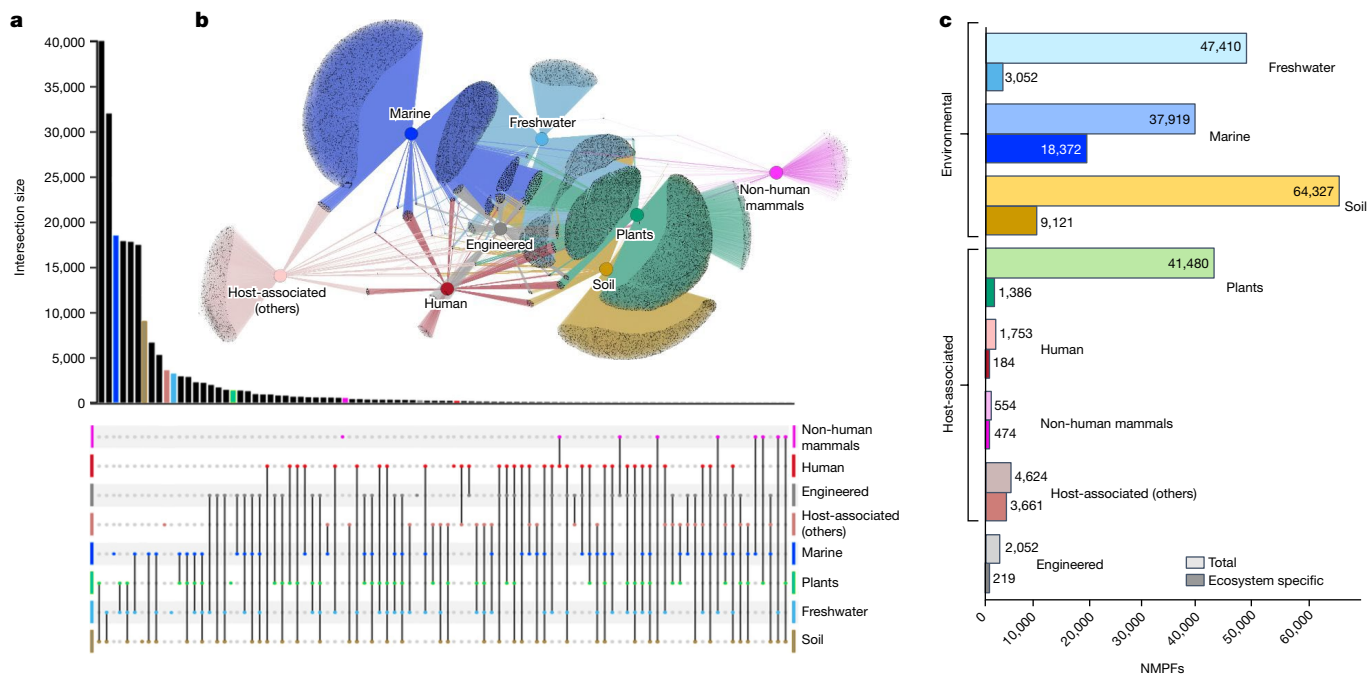


Fig. 2 | Ecosystem analysis of NMPFs. **a**, UpSet plot representation of protein clusters overlapping across the eight ecosystem types. The various intersections among different categories are represented by the chart at the bottom, with each category shown as a dot and intersecting categories connected by straight lines. The sizes of the intersection sets are represented by the vertical bar chart. Intersection sets of 15 NMPFs or higher are shown.

b, Network representation of the protein clusters and their ecosystems. Eight ecosystem types were applied according to the GOLD ecosystem classification, represented by central, coloured nodes (hubs), whereas the grey peripheral nodes represent the protein clusters. The edges represent the protein cluster–ecosystem associations. **c**, The distribution of total versus ecosystem-type-specific NMPFs across the eight different ecosystem types.

associated with each ecosystem type. The only exception was the non-human-mammal-associated NMPFs, for which prevalence reached up to around 45% of the total non-human mammalian datasets.

Taxonomic distribution

Taxonomic assignment of NMPFs was performed on the basis of the available taxonomy information of the corresponding scaffolds in IMG, for each member of the clusters¹⁸. In cases in which no such annotation was available, we used a combination of additional approaches to computationally infer the taxonomy of the scaffolds (Methods). Of the total 17,280,119 IMG/M scaffolds containing the NMPF members, 8,049,154 were classified as Bacteria, 382,761 as Archaea, 1,184,393 as Eukaryota and 1,406,588 as viruses, leaving 6,257,223 as unclassified.

The taxonomic distribution of the NMPFs, on the basis of their corresponding scaffold taxonomic assignment, is shown in Fig. 3a and Extended Data Fig. 6. The majority of protein families included sequences with multiple taxonomic assignments (such as bacterial and unclassified, or bacterial and viral). The largest category consisted of families with bacterial/unclassified sequences, followed by viruses/unclassified and bacteria/viruses. A much smaller group of families was assigned to Eukarya and even fewer families to Archaea. Finally, 7,253 clusters had no taxonomic information at all.

As no reliable de novo eukaryotic gene predictor exists for unbinned metagenomes¹⁹, a lot of sequences may come from eukaryotic scaffolds that may contain translation errors (such as mistranslated introns). However, analysing the contents of these clusters (Supplementary Methods) showed that their majority include proteins from Bacteria and Archaea alongside Eukarya, with very few NMPFs containing only eukaryotic sequences (Supplementary Data 6). Moreover, more than half of these clusters are validated by metatranscriptomic data. These two observations supported the quality of the eukaryotic-containing NMPFs.

Subsequently, we evaluated whether any of the NMPF proteins (and their corresponding families) were found in any of the recently identified MAGs from the Genomes from Earth’s Microbiomes (GEM) catalogue²⁰. Specifically, we examined whether any of the scaffolds containing genes of the NMPFs were binned in any of the 52,515 MAGs of the GEM catalogue. This revealed that only 17,953 genes, coming from 7,937 NMPFs (7.4% of total) (Fig. 3b,c), were found within the GEM catalogue, of which the vast majority (93%) was from uncultured species. For those families that were present in two or more MAGs, we noticed a strong narrow taxonomic distribution, with more than two-thirds being restricted to a single species or genus, and only a very small number found across multiple families, classes or phyla (Fig. 3d). NMPFs were found to be statistically enriched in several phyla common in soil environments (for example, Gemmatimonadota, Acidobacteriota, Crenarchaeota and Myxococcota) and statistically depleted from several phyla found in humans and other host-associated environments (Firmicutes, Proteobacteria and Bacteroidota; Fig. 3e). Taken together, these results reveal that a significant fraction of functional diversity remains taxonomically orphan despite improvements in sequencing throughout and large-scale MAG reconstructions.

Metadata distribution

We next examined the geographical distribution of NMPFs (Extended Data Fig. 7). A very small number of families (1,372; 1.3%) was found to have limited geographical distribution (within 1 km), and this number only moderately increased (4,330; 4%) when we allowed for a maximum distance of 1,000 km. Most of these families were found in plant, soil and freshwater ecosystems. A very small number of these families included members found in marine ecosystems or human samples as expected from the higher microbial dispersal in these ecosystems (Extended Data Fig. 7f,g).

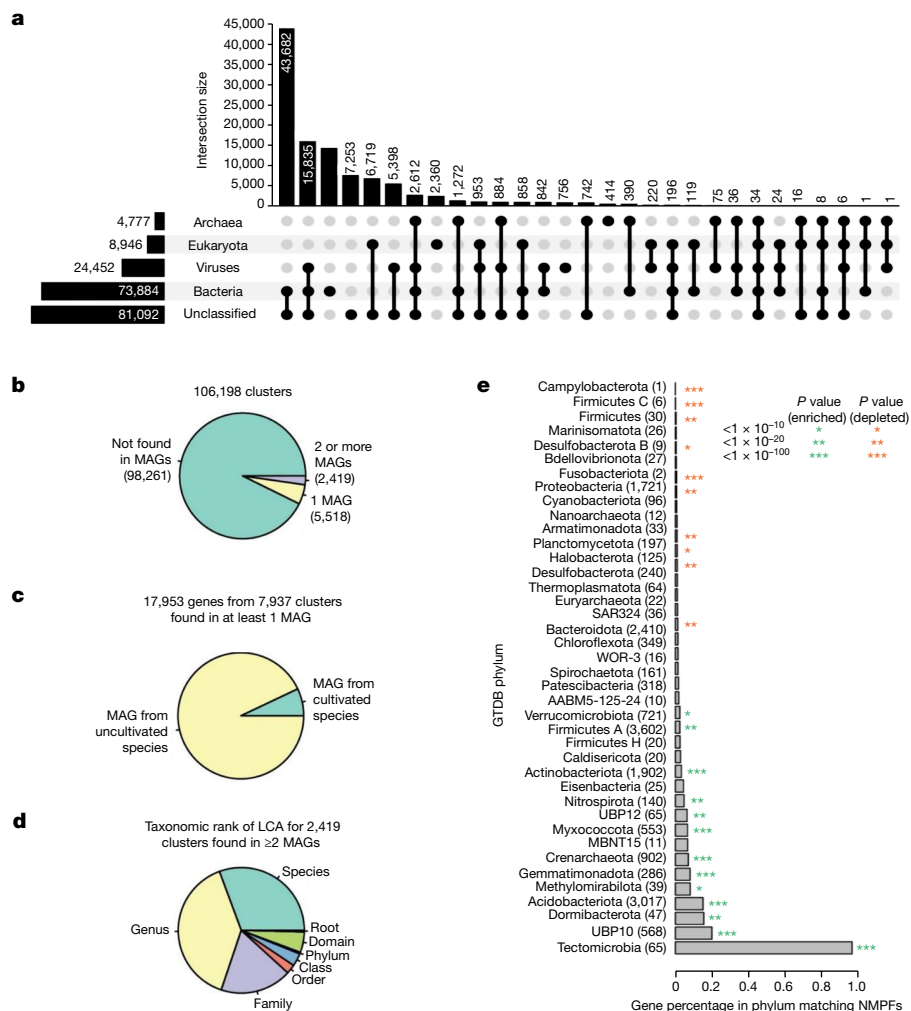


Fig. 3 | Taxonomic composition and occurrence of NMPFs in bacterial and archaeal MAGs. **a**, UpSet plot showing the domain-level taxonomic distribution of novel protein clusters. The total size of each taxonomic category is represented through the horizontal bar chart on the left. The intersections among categories are represented by the chart at the bottom, with sizes of the intersections represented by the vertical bar chart at the top. **b,c**, We determined whether NMPFs were found on scaffolds from the GEM

The majority of NMPFs (64,186 or 60.44%) comprised a mixture of proteins from both metagenomes and metatranscriptomes, further validating their existence, whereas 38,292 (36.06%) of NMPFs contained proteins found exclusively in metagenomes and 3,720 (3.50%) of NMPFs contained proteins found only in metatranscriptomes (Supplementary Table 5). The percentage of families containing members from both metagenomes and metatranscriptomes steadily decreased along with the number of members per family. NMPFs found in both metagenomes and metatranscriptomes also had the widest sample distribution, that is, the clusters were found in the largest numbers of samples (Supplementary Table 6). The majority of these clusters was classified in environmental ecosystems (soil and, to a lesser extent, marine and freshwater samples) and primarily contained bacterial and unclassified sequences.

To estimate the distribution of novel protein clusters among the environmental sequencing data, we compared the number of novel proteins, extracted from each scaffold and used in this study, against the total number of genes/proteins in the respective scaffold. Most analysed scaffolds (13,407,728 or 77.59%) contained both novel and known genes (top 20 scaffolds; Supplementary Tables 7–11). A comparison of novel versus the total number of genes in these scaffolds revealed that

catalogue (**b**) and whether they were found on scaffolds from one or more cultivated species (**c**). **d**, The taxonomic rank of the lowest common ancestor (LCA) for 2,419 clusters found in at least 2 MAGs. **e**, The percentage of genes matching a cluster from MAGs assigned to different phyla. The asterisks indicate significant *P* values from a hypergeometric test. Green, clusters enriched in the phylum; red, clusters depleted from the phylum. The number of genes matching clusters is indicated in parenthesis next to the phylum name.

the size of the scaffold or total number of genes per scaffold was not correlated with the number of novel genes. The largest scaffold in our study (5,123,848 bp, 4,302 genes) contained only one novel sequence. Generally, the largest scaffolds in the study contained only a limited number of novel sequences and originated from bacterial or unclassified metagenomic samples (Supplementary Table 9). Conversely, the scaffolds with the most novel sequences were of variable length (and gene count) and mostly originated from viruses (Supplementary Table 10).

As the majority of novel proteins (14,185,414 sequences) was located next to known genes, we investigated the co-occurrence of NMPFs with neighbouring genes assigned to the same Pfam family. Additional annotation was obtained by mapping each NMPF's co-occurring Pfam domains to their corresponding COG functional categories; this can be used to provide further information on each family's gene neighbourhood. The distribution of NMPFs across functional categories is given in Supplementary Figs. 3–5. Conserved gene neighbourhoods suggest functional coupling²¹ and can therefore be used to provide additional lines of information for putative function prediction. Accordingly, family F004468 was found to co-occur with ribosomal proteins in 78% of scaffolds (that is, in 118 scaffolds out of the 151 scaffolds in which it

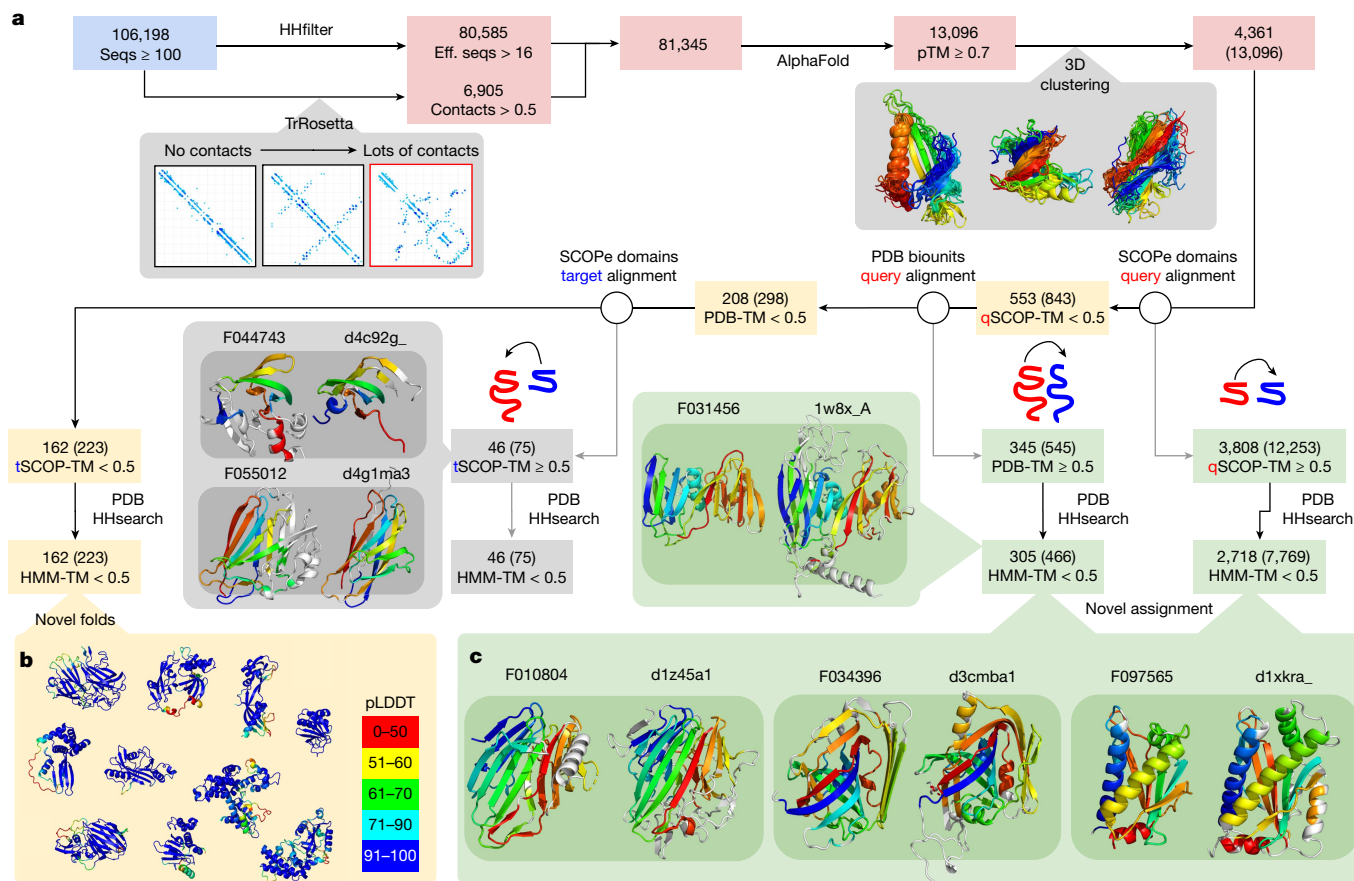


Fig. 4 | Structural characterization of the NMPFs. **a**, Protein clusters with at least 16 effective sequences (eff. seqs) or many contacts were submitted to AlphaFold. The results were filtered to include structures with high predicted confidence (pTM ≥ 0.70), which were then clustered on the basis of pairwise TM-score calculation. All of the subsequent steps of the workflow display the number of unique clusters followed by the total number of NMPFs in parentheses. As filtering was performed at the NMPF level, only the numbers in parentheses will sum, as it is possible for members of the same cluster to fall on different sides of each TM-score filtering step. Each predicted structure was aligned against SCOPe domains. Models with no hits to SCOPe were further

aligned and filtered if there were any hits to full PDB assemblies or one of the SCOPe domains aligned to at least 50% of the predicted structure. The domains (from SCOPe matches) or multi-domain (from PDB matches) were further screened using HHsearch against the PDB. The PDB of the top hit was compared to the prediction. **b**, Models with no significant hits to either SCOPe or PDB were considered to be potential novel folds. pLDDT, per-residue confidence score. **c**, Models with hits to either SCOPe domains or PDB biological assemblies with no significant HHsearch hits (HMM-TM-score < 0.5) were considered to be novel assignments.

was encoded), suggesting that it has a translation-related function. Similarly, family F021307 was found within a probable chloroplast ribosomal protein operon in 67% of encoding scaffolds. In total, 7,625 NMPFs were found to have greater than 50% co-occurrence with specific Pfams, while 585 families had greater than 90% co-occurrence with a Pfam family (Supplementary Data 1). These associations can also be used to predict a functional role for NMPFs; a few examples are given in Extended Data Figs. 8 and 9, in which the gene neighbourhoods of selected NMPFs are presented as association networks, combined with functional annotation from COG.

Structural distribution

Recent breakthroughs in protein structure prediction²² have enabled fast and accurate structural characterization of protein sequences. Metagenomic sequences have been shown to represent a particularly rich source for the discovery of novel structures^{23,24}. Here we ran AlphaFold2²² on NMPFs with at least 16 diverse sequences, or where TrRosetta²⁵ predicted a well-structured protein (Methods). The results are summarized in Fig. 4a. Out of the 81,345 NMPFs that met the above criteria, 80,585 3D models were predicted, with 13,096 NMPFs having a

high confidence (predicted TM (pTM) score > 0.700) prediction. The pTM-score integrates both the predicted confidence per position and the predicted alignment error (pAE) for every pair of positions, indicating the confidence of domain–domain orientations.

On the basis of structural clustering, these high-confidence predictions represented 4,361 unique structures. To examine the novelty or functions of these structures, we compared them to experimentally determined structures from SCOP-Extended (SCOPe)²⁶ and assemblies from the Protein Data Bank (PDB)²⁷. In total, 3,808 structures (12,253 NMPFs) had a significant structural overlap with at least 1 SCOPe domain (TM-score > 0.5). Of these, 2,718 (7,769 NMPFs) had a non-trivial hit, indicating that 62.3% of high-quality predictions had some similarity to at least one SCOPe domain or PDB assembly.

These novel assignments, based on structural similarity, can now be used for functional prediction of the corresponding sequences. A few examples are shown in Fig. 4c. For example, family F034396 had no hits to the PDB using HHsearch (top hit of *e*-value = 12), yet a strong hit to the PDB using a structural search of the SCOPe domain d3cmba1 (TM-score = 0.69), with the function of acetoacetate decarboxylase. Other examples with no HHsearch hits (*e*-value > 10), yet strong structural hits included F010804-d1z45a1 (TM-score = 0.73, galactose

mutarotase) and F097565-d1xkra_ (TM-score = 0.73, chemotaxis). We stress that these cases should be treated as informed predictions that require experimental validation, as the same fold does not always correspond to the same function. A full list is provided in Supplementary Data 2. However, some validation and additional functional annotation can be performed by combining these novel assignments with other NMPF metadata, such as gene co-occurrence. A few examples are given in Extended Data Fig. 8.

To confirm that the remaining 553 proteins with no SCOPe hit were novel folds, a more thorough search was performed against all PDB biological assemblies, including all possible chain permutations. In total, 345 models had a hit to at least one PDB entry, of which 305 represented additional novel assignments. The remaining 208 were processed for further filtering, removing predictions of which 50% of the structure matched a SCOPe domain. Finally, 162 folds and/or domain–domain orientations from 223 NMPFs were identified as novel (Fig. 4b). A complete list of these folds is provided in Supplementary Data 3.

Although the absence of any significant structural homology precludes the reliable functional annotation for these novel folds, some hints towards their potential function can be gleaned from their associated metadata. Characteristic examples are given in Extended Data Fig. 9, showcasing the gene neighbourhood and ecosystem metadata of three NMPFs with novel structural folds.

Discussion

Arguably, the best approach for estimating and exploring microbial functional diversity is through systematically cataloguing and exhaustively characterizing sequence-diversity space. Over the past three decades, genome sequencing of hundreds of thousands of cultured microbial strains has enabled unprecedented growth and characterization of this sequence space, revealing that sequencing efforts targeted to maximize phylogenetic diversity can lead to further discoveries and growth of currently known protein family diversity²⁸. Although the exploration of the corresponding sequence-encoded functional diversity is lagging substantially²⁹, the explosion in the number of identified novel protein families has, to a great extent, been accompanied by an increase in targeted functional characterization of some of those families, particularly in areas of important biotechnological applications such as the discovery of new CRISPR–Cas genes and systems³⁰. The advent of metagenomics has further fuelled the rush to discover new enzymatic activities by unearthing a hidden treasure trove of untapped sequence information. Yet, aside from generating for-the-first-time important habitat-specific environmental gene catalogues³¹, most explorations of exponentially growing metagenomic sequence space have focused on expanding the diversity and characterization of previously known protein families³².

To alleviate this limitation and pioneer global insights into the extent of novel sequence space and, by effect, functional diversity across the realm of sequenced biomes, we have amassed close to 27,000 publicly available assembled metagenomic and metatranscriptomic datasets. From these datasets, we generated the NMPF catalogue, consisting of 106,198 metagenome protein families of 100 members or more with no sequence similarity to genes from reference microbial genomes or Pfam entries. Although these families represented a mere duplication over the number of families generated from more than 100,000 reference genomes integrated into IMG from all domains of life, far greater increases were observed in the families containing more than 25, 50 or 75 members, strongly suggesting that extensive sequence and functional diversity remains untapped. We anticipate that this diversity in unexplored microbial protein space will continue to increase over the next several years as more novel environmental samples are sequenced.

Although a much smaller number of metatranscriptomes was available for this analysis (4,739; 17.6%), we observed that the majority of

NMPFs (60%) comprised proteins encoded by genes identified in both metagenomes and metatranscriptomes, indicating that most of those genes are actively expressed, further supporting the validity of those clusters. The clustering quality was also supported by the observation that 92% of clusters had members spanning 50 samples or more, while 50% of the clusters were from proteins distributed across 100 samples or more (Fig. 2d).

The identification of 7.5% of the NMPFs on the recently reconstructed MAGs of the GEM catalogue indicates that, as we continue to access the genetic content of uncultured microbial diversity, an increasing number of taxonomically orphan novel protein families will become taxonomically assigned, an important step towards their functional and ecological characterization.

There are several limitations underlying the metagenomic data and methodology used in this study. One limiting factor to consider is the short size (shorter than 5 kb) of the majority of scaffolds used in this study. However, note that, due to the required alignment coverage of at least 80%, potentially truncated sequences have to be sufficiently complete to cluster with full-length sequences (defined as located in the middle of longer scaffolds). This requirement has largely precluded the enrichment of NMPFs with fragmented proteins. However, even in the case of NMPFs with a high percentage of these suspect sequences, the clusters are found to produce stable 3D models (often with high structural quality, as evidenced by pLDDT and pTM scores), many of which have structural homologues to SCOPe domains. As a result, families containing such sequences could potentially represent protein fragments or protein domains that form parts of multi-domain sequences, or components in multimeric complexes. An additional potential limitation is the inclusion of eukaryotic sequences in the sequence dataset, which may introduce errors in the analysis. Yet, as shown (taxonomic distribution; Supplementary Methods), the contributions from eukaryotic scaffolds are relatively small, and the majority of the associated NMPFs also contain data from metatranscriptomes and/or prokaryotic taxa in sequence alignments, supporting their validity. However, until reliable eukaryotic gene predictors for metagenomes become available, eukaryotic, as well as unclassified NMPFs and sequences should be handled with care.

Overall, as more metagenomic data become available, an increasing diversity of sequences will be incorporated into NMPFs, which will then enable the generation of a much higher number of high-confidence structures, and therefore further increase the numbers of assignments to known structures as well as uncover novel folds. The identification of NMPFs opens new paths for structural genomics and challenges for fold recognition and the exploration of microbial dark matter.

Online content

Any methods, additional references, Nature Portfolio reporting summaries, source data, extended data, supplementary information, acknowledgements, peer review information; details of author contributions and competing interests; and statements of data and code availability are available at <https://doi.org/10.1038/s41586-023-06583-7>.

1. New, F. N. & Brito, I. L. What is metagenomics teaching us, and what is missed? *Annu. Rev. Microbiol.* **74**, 117–135 (2020).
2. Rinke, C. et al. Insights into the phylogeny and coding potential of microbial dark matter. *Nature* **499**, 431–437 (2013).
3. Mistry, J. et al. Pfam: the protein families database in 2021. *Nucleic Acids Res.* **49**, D412–D419 (2021).
4. Meyer, F. et al. MG-RAST version 4—lessons learned from a decade of low-budget ultra-high-throughput metagenome analysis. *Brief. Bioinform.* **20**, 1151–1159 (2019).
5. Ayling, M., Clark, M. D. & Leggett, R. M. New approaches for metagenome assembly with short reads. *Brief. Bioinform.* **21**, 584–594 (2020).
6. Chen, I.-M. A. et al. The IMG/M data management and analysis system v.6.0: new tools and advanced capabilities. *Nucleic Acids Res.* **49**, D751–D763 (2021).
7. Mitchell, A. L. et al. MGnify: the microbiome analysis resource in 2020. *Nucleic Acids Res.* **48**, D570–D578 (2019).
8. Galperin, M. Y. et al. COG database update: focus on microbial diversity, model organisms, and widespread pathogens. *Nucleic Acids Res.* **49**, D274–D281 (2021).

9. Kanehisa, M., Sato, Y., Kawashima, M., Furumichi, M. & Tanabe, M. KEGG as a reference resource for gene and protein annotation. *Nucleic Acids Res.* **44**, D457–D462 (2016).
10. Vanni, C. et al. AGNOSTOS-DB: a resource to unlock the uncharted regions of the coding sequence space. Preprint at *bioRxiv* <https://doi.org/10.1101/2021.06.07.447314> (2021).
11. Rodriguez del Rio, Á. et al. Functional and evolutionary significance of unknown genes from uncultivated taxa. Preprint at *bioRxiv* <https://doi.org/10.1101/2022.01.26.477801> (2022).
12. Modha, S., Robertson, D. L., Hughes, J. & Orton, R. J. Quantifying and cataloguing unknown sequences within human microbiomes. *mSystems* <https://doi.org/10.1128/msystems.01468-21> (2022).
13. Azad, A., Pavlopoulos, G. A., Ouzounis, C. A., Kyripides, N. C. & Buluç, A. HipMCL: a high-performance parallel implementation of the Markov clustering algorithm for large-scale networks. *Nucleic Acids Res.* **46**, e33 (2018).
14. Enright, A. J., Van Dongen, S. & Ouzounis, C. A. An efficient algorithm for large-scale detection of protein families. *Nucleic Acids Res.* **30**, 1575–1584 (2002).
15. Mukherjee, S. et al. Genomes OnLine Database (GOLD) v.8: overview and updates. *Nucleic Acids Res.* **49**, D723–D733 (2021).
16. Ivanova, N. et al. A call for standardized classification of metagenome projects. *Environ. Microbiol.* **12**, 1803–1805 (2010).
17. Nayfach, L. P. et al. Towards the biogeography of prokaryotic genes. *Nature* **601**, 252–256 (2022).
18. Clum, A. et al. DOE JGI Metagenome Workflow. *mSystems* **6**, e00804-20 (2021).
19. Baltoumas, F. A. et al. Exploring microbial functional biodiversity at the protein family level: From metagenomic sequence reads to annotated protein clusters. *Front. Bioinform.* **3**, 1157956 (2023).
20. Nayfach, S. et al. A genomic catalog of Earth's microbiomes. *Nat. Biotechnol.* **39**, 499–509 (2021).
21. Overbeek, R., Fonstein, M., D'Souza, M., Pusch, G. D. & Maltsev, N. The use of gene clusters to infer functional coupling. *Proc. Natl Acad. Sci. USA* **96**, 2896–2901 (1999).
22. Jumper, J. et al. Highly accurate protein structure prediction with AlphaFold. *Nature* **596**, 583–589 (2021).
23. Ovchinnikov, S. et al. Protein structure determination using metagenome sequence data. *Science* **355**, 294–298 (2017).
24. Hou, Q. et al. Using metagenomic data to boost protein structure prediction and discovery. *Comput. Struct. Biotechnol. J.* **20**, 434–442 (2022).
25. Yang, J. et al. Improved protein structure prediction using predicted interresidue orientations. *Proc. Natl Acad. Sci. USA* **117**, 1496–1503 (2020).
26. Chandonia, J.-M. et al. SCOPe: improvements to the structural classification of proteins—extended database to facilitate variant interpretation and machine learning. *Nucleic Acids Res.* **50**, D553–D559 (2022).
27. Berman, H., Henrick, K. & Nakamura, H. Announcing the worldwide Protein Data Bank. *Nat. Struct. Biol.* **10**, 980 (2003).
28. Mukherjee, S. et al. 1,003 reference genomes of bacterial and archaeal isolates expand coverage of the tree of life. *Nat. Biotechnol.* **35**, 676–683 (2017).
29. Roberts, R. J. et al. COMBREX: a project to accelerate the functional annotation of prokaryotic genomes. *Nucleic Acids Res.* **39**, D11–D14 (2011).
30. Koonin, E. V. & Makarova, K. S. Evolutionary plasticity and functional versatility of CRISPR systems. *PLoS Biol.* **20**, e3001481 (2022).
31. Qin, J. et al. A human gut microbial gene catalogue established by metagenomic sequencing. *Nature* **464**, 59–65 (2010).
32. Wyman, S. K., Avila-Herrera, A., Nayfach, S. & Pollard, K. S. A most wanted list of conserved microbial protein families with no known domains. *PLoS ONE* **13**, e0205749 (2018).

Publisher's note Springer Nature remains neutral with regard to jurisdictional claims in published maps and institutional affiliations.



Open Access This article is licensed under a Creative Commons Attribution 4.0 International License, which permits use, sharing, adaptation, distribution and reproduction in any medium or format, as long as you give appropriate credit to the original author(s) and the source, provide a link to the Creative Commons licence, and indicate if changes were made. The images or other third party material in this article are included in the article's Creative Commons licence, unless indicated otherwise in a credit line to the material. If material is not included in the article's Creative Commons licence and your intended use is not permitted by statutory regulation or exceeds the permitted use, you will need to obtain permission directly from the copyright holder. To view a copy of this licence, visit <http://creativecommons.org/licenses/by/4.0/>.

© The Author(s) 2023

Novel Metagenome Protein Families Consortium

Silvia G. Acinas¹⁷, Nathan Ahlgren¹⁸, Graeme Attwood¹⁹, Petr Baldrian²⁰, Timothy Berry²¹, Jennifer M. Bhatnagar²², Devaki Bhaya²³, Kay D. Bidle²⁴, Jeffrey L. Blanchard²⁵, Eric S. Boyd²⁶, Jennifer L. Bowen²⁷, Jeff Bowman²⁸, Susan H. Brawley²⁹, Eoin L. Brodie³⁰, Andreas Brune³¹, Donald A. Bryant³², Alison Buchan³³, Hinsby Cadillo-Quiroz³⁴, Barbara J. Campbell³⁵, Ricardo Cavicchioli³⁶, Peter F. Chuckran³⁷, Maureen Coleman³⁸, Sean Crowe³⁹, Daniel R. Colman⁴⁰, Cameron R. Currie⁴¹, Jeff Dangl⁴², Nathalie Delherbe⁴⁰, Vincent J. Denef⁴³, Paul Dijkstra³⁷, Daniel D. Distel⁴⁴, Emiley Eloë-Fadrosh², Kirsten Fisher⁴⁵, Christopher Francis⁴⁶, Aaron Garoutte³, Amelie Gaudin⁴⁷, Lena Gerwick⁴⁸, Filipa Godoy-Vitorino⁴⁹, Peter Guerra⁵⁰, Jiarong Guo⁹, Mussie Y. Habteselassie⁵¹, Steven J. Hallam⁵², Roland Hatzenpichler⁵³, Ute Hentschel⁵⁴, Matthias Hess⁵⁵, Ann M. Hirsch⁵⁶, Laura A. Hug⁵⁷, Jenni Hultman⁵⁸, Dana E. Hunt⁵⁹, Marcel Huntemann², William P. Inskeep⁶⁰, Timothy Y. James⁴³, Janet Jansson⁶¹, Eric R. Johnston⁶²,

Marina Kalyuzhnaya⁴², Charlene N. Kelly⁶³, Robert M. Kelly⁶⁴, Jonathan L. Klassen⁶⁵, Klaus Nüsslein⁶⁶, Joel E. Kostka⁶⁷, Steven Lindow⁶⁸, Erik Lilleskov⁶⁹, Mackenzie Lynes⁵³, Rachel Mackelprang⁷⁰, Francis M. Martin⁷¹, Olivia U. Mason⁷², R. Michael McKay⁷³, Katherine McMahon⁷⁴, David A. Mead⁷⁵, Monica Medina⁷⁶, Laura K. Meredith^{77,78}, Thomas Mock⁷⁹, William W. Mohn⁸⁰, Mary Ann Moran⁸¹, Alison Murray⁸², Josh D. Neufeld⁵⁷, Rebecca Neumann⁸³, Jeanette M. Norton⁸⁴, Laila P. Partida-Martinez⁸⁵, Nicole Pietrasiak⁸⁶, Dale Pelletier⁸², T. B. K. Reddy², Brandi Kiel Reese⁸⁷, Nicholas J. Reichart⁸³, Rebecca Reiss⁸⁸, Mak A. Saito⁸⁹, Daniel P. Schachtman⁹⁰, Rekha Seshadri², Ashley Shade⁹¹, David Sherman^{92,93}, Rachel Simister⁸⁰, Holly Simon^{94,95}, James Stegen⁸⁶, Ramunas Stepanauskas⁹⁷, Matthew Sullivan⁹⁸, Dawn Y. Sumner⁹⁹, Hanno Teeling¹⁰⁰, Kimberlee Thamatrakoln²⁴, Kathleen Treseder¹⁰¹, Susannah Tringe², Parag Vaishampayan¹⁰², David L. Valentine¹⁰³, Nicholas B. Waldo⁸³, Mark P. Waldrop¹⁰⁴, David A. Walsh¹⁰⁵, David M. Ward⁶⁰, Michael Wilkins¹⁰⁶, Thea Whitman²¹, Jamie Woollet¹⁰⁷ & Tanja Woyke²

¹⁷Department of Marine Biology and Oceanography, Institut de Ciències del Mar, Barcelona, Spain. ¹⁸Biology Department, Clark University, Worcester, MA, USA. ¹⁹AgResearch, Grasslands Research Centre, Palmerston North, New Zealand. ²⁰Laboratory of Environmental Microbiology, Institute of Microbiology of the Czech Academy of Sciences, Prague, Czech Republic. ²¹Department of Soil Science, University of Wisconsin-Madison, Madison, WI, USA. ²²Department of Biology, Boston University, Boston, MA, USA. ²³Carnegie Institution for Science, Stanford, CA, USA. ²⁴Department of Marine and Coastal Sciences, Rutgers University, New Brunswick, NJ, USA. ²⁵Department of Biology, University of Massachusetts, Amherst, MA, USA. ²⁶Department of Microbiology and Cell Biology, Montana State University, Bozeman, MT, USA. ²⁷Marine Science Center, Department of Marine and Environmental Sciences, Northeastern University, Nahant, MA, USA. ²⁸Integrative Oceanography Division, Scripps Institution of Oceanography, UC San Diego, La Jolla, CA, USA. ²⁹School of Marine Sciences, University of Maine, Orono, ME, USA. ³⁰Earth and Environmental Sciences, Lawrence Berkeley National Laboratory, Berkeley, CA, USA. ³¹Research Group Insect Microbiology and Symbiosis, Max Planck Institute for Terrestrial Microbiology, Marburg, Germany. ³²Department of Biochemistry and Molecular Biology, The Pennsylvania State University, University Park, PA, USA. ³³Department of Microbiology, The University of Tennessee, Knoxville, Knoxville, TN, USA. ³⁴School of Life Sciences, Arizona State University, Tempe, AZ, USA. ³⁵Department of Biological Sciences, Clemson University, Clemson, SC, USA. ³⁶School of Biotechnology and Biomolecular Sciences, UNSW Sydney, Sydney, New South Wales, Australia. ³⁷Center for Ecosystem Science and Society, Northern Arizona University, Flagstaff, AZ, USA. ³⁸Department of the Geophysical Sciences, University of Chicago, Chicago, IL, USA. ³⁹Department of Microbiology and Immunology, University of British Columbia, Vancouver, British Columbia, Canada. ⁴⁰Department of Biology, San Diego State University, San Diego, CA, USA. ⁴¹Department of Bacteriology, University of Wisconsin-Madison, Madison, WI, USA. ⁴²Department of Biology, University of North Carolina at Chapel Hill, Chapel Hill, NC, USA. ⁴³Department of Ecology and Evolutionary Biology, University of Michigan, Ann Arbor, MI, USA. ⁴⁴Ocean Genome Legacy, Marine Science Center, Northeastern University, Nahant, MA, USA. ⁴⁵Department of Biological Sciences, California State University, Los Angeles, CA, USA. ⁴⁶Department of Earth System Science, Stanford University, Stanford, CA, USA. ⁴⁷Department of Plant Sciences, University of California, Davis, Davis, CA, USA. ⁴⁸Center for Marine Biotechnology and Biomedicine, Scripps Institution of Oceanography, University of California San Diego, La Jolla, CA, USA. ⁴⁹Department of Microbiology and Medical Zoology, School of Medicine, University of Puerto Rico, San Juan, PR, USA. ⁵⁰Lynker, Albuquerque, NM, USA. ⁵¹Department of Crops and Soil Sciences, University of Georgia, Griffin, GA, USA. ⁵²Department of Microbiology & Immunology, University of British Columbia, Vancouver, British Columbia, Canada. ⁵³Department of Chemistry and Biochemistry, Montana State University, Bozeman, MT, USA. ⁵⁴RD3 Marine Symbioses, GEOMAR Helmholtz Centre for Ocean Research Kiel, Kiel, Germany. ⁵⁵Systems Microbiology and Natural Products Laboratory, University of California, Davis, Davis, CA, USA. ⁵⁶Department of Molecular, Cell & Developmental Biology, University of California, Los Angeles (UCLA), Los Angeles, CA, USA. ⁵⁷Department of Biology, University of Waterloo, Waterloo, Ontario, Canada. ⁵⁸Department of Microbiology, University of Helsinki, Helsinki, Finland. ⁵⁹Marine Laboratory, Duke University, Beaufort, NC, USA. ⁶⁰Department of Land Resources & Environmental Sciences, Montana State University, Bozeman, MT, USA. ⁶¹Earth and Biological Sciences Directorate, Pacific Northwest National Lab, Richland, WA, USA. ⁶²Biosciences Division, Oak Ridge National Laboratory, Oak Ridge, TN, USA. ⁶³Division of Forestry and Natural Resources, West Virginia University, Morgantown, WV, USA. ⁶⁴Department of Chemical and Biomolecular Engineering, North Carolina State University, Raleigh, NC, USA. ⁶⁵Department of Molecular and Cell Biology, University of Connecticut, Storrs, CT, USA. ⁶⁶Department of Microbiology, University of Massachusetts Amherst, Amherst, MA, USA. ⁶⁷School of Biological Sciences, Georgia Institute of Technology, Atlanta, GA, USA. ⁶⁸Department of Plant and Microbial Biology, University of California, Berkeley, CA, USA. ⁶⁹USDA Forest Service, Northern Research Station, Houghton, MI, USA. ⁷⁰Department of Biology, California State University Northridge, Northridge, CA, USA. ⁷¹Université de Lorraine, INRAE, UMR 1136 Interactions Arbres/Microorganismes, INRAE-Grand Est-Nancy, Champenoux, France. ⁷²Department of Earth, Ocean and Atmospheric Science, Florida State University, Tallahassee, FL, USA. ⁷³Great Lakes Institute for Environmental Research, University of Windsor, Windsor, Ontario, Canada. ⁷⁴Departments of Civil and Environmental Engineering and Bacteriology, University of Wisconsin, Madison, WI, USA. ⁷⁵Varigen Biosciences Corporation, Madison, WI, USA. ⁷⁶Biology Department, The Pennsylvania State University, University Park, PA, USA. ⁷⁷School of Natural Resources and the Environment, University of Arizona, Tucson, AZ, USA. ⁷⁸BIO5 Institute, University of Arizona, Tucson, AZ, USA. ⁷⁹School of Environmental Sciences, University of East Anglia, Norwich, UK. ⁸⁰Department of Microbiology & Immunology, Life Sciences Institute, The University of British Columbia, Vancouver, British Columbia, Canada. ⁸¹Department of Marine Sciences, University of Georgia, Athens, GA, USA. ⁸²Division of Earth and Ecosystem Science, Desert Research Institute, Reno, NV, USA. ⁸³Department of Civil & Environmental Engineering, University of Washington, Seattle, WA, USA. ⁸⁴Department of Plants, Soils and Climate, Utah State University, Logan, UT, USA. ⁸⁵Unidad Irapuato, Centro de Investigación y de Estudios Avanzados del IPN (Cinvestav), Irapuato, Mexico. ⁸⁶Plant and Environmental Sciences Department, New Mexico State University, Las Cruces, NM, USA. ⁸⁷University of South Alabama, Mobile, AL, USA. ⁸⁸New Mexico Institute of Mining and Technology, Socorro, NM, USA. ⁸⁹Marine Chemistry and

Article

Geochemistry Department, Woods Hole Oceanographic Institution, Woods Hole, MA, USA. ⁹⁰Department of Agronomy and Horticulture and Center for Plant Science Innovation, University of Nebraska–Lincoln, Lincoln, NE, USA. ⁹¹Department of Microbiology and Molecular Genetics, Michigan State University, East Lansing, MI, USA. ⁹²Life Sciences Institute, University of Michigan, Ann Arbor, MI, USA. ⁹³Departments of Medicinal Chemistry, Chemistry, and Microbiology and Immunology, University of Michigan, Ann Arbor, MI, USA. ⁹⁴Division of Environmental and Biomolecular Systems, Institute of Environmental Health, Oregon Health & Science University, Portland, OR, USA. ⁹⁵Animal Microbiome Analytics, Oakland, CA, USA. ⁹⁶Pacific Northwest National Laboratory, Richland, WA, USA. ⁹⁷Bigelow Laboratory for Ocean Sciences, East Boothbay, ME, USA. ⁹⁸Departments of Microbiology and Civil, Environmental

and Geodetic Engineering, Ohio State University, Columbus, OH, USA. ⁹⁹Department of Earth and Planetary Sciences, University of California Davis, Davis, CA, USA. ¹⁰⁰Max-Planck-Institute for Marine Microbiology, Bremen, Germany. ¹⁰¹Department of Ecology and Evolutionary Biology, University of California Irvine, Irvine, CA, USA. ¹⁰²Space Biosciences Division, NASA Ames Research Center, Moffett Field, CA, USA. ¹⁰³Department of Earth Science and Marine Science Institute, University of California, Santa Barbara, CA, USA. ¹⁰⁴Geology, Minerals, Energy and Geophysics Science Center, Menlo Park, CA, USA. ¹⁰⁵Department of Biology, Concordia University, Montreal, Quebec, Canada. ¹⁰⁶Department of Soil & Crop Sciences, Colorado State University, Fort Collins, CO, USA. ¹⁰⁷Department of Forest and Rangeland Stewardship, Colorado State University, Fort Collins, CO, USA

Methods

Data collection and filtering

All publicly available metagenomes, metatranscriptomes and reference genomes were retrieved from the IMG/M database⁶ (database release, July 2019). Low-complexity regions were removed with the use of the tantan application³³. In total, we extracted all protein sequences from 89,412 bacterial, 9,202 viral, 3,073 archaeal and 804 eukaryal genomes. This corresponded to 87,084,214 bacterial, 221,027 viral, 2,464,569 archaeal and 4,902,193 eukaryotic non-redundant proteins, resulting in a final dataset of 94,672,003 sequences. Pfam hits (v.31) were detected with the use of the hmsearch tool (HMMER v.3.1 package)³⁴ using the default trusted cut-off. Hits to proteins from reference genomes were calculated using LAST³⁵. We considered a hit to be any aligned sequence at >30% identity over 70% of its length (bidirectionally between the query and the subject). A detailed workflow of the sequence selection, filtering and analysis procedure is provided in the Supplementary Methods. A full summary of the sequences contained in each metagenome and metatranscriptome dataset, including hits to Pfam and reference genomes, sequences used in clustering (see below) and the remaining unannotated sequences, is provided in Supplementary Data 4.

Sequence clustering and analysis

Sequence clustering was performed using the HipMCL algorithm with inflation parameter 2.0 using identity scores as the input. HipMCL was chosen over other clustering solutions owing to its scalability and parallelization capabilities, as well as its ability to efficiently cluster very large datasets (Supplementary Methods). Before clustering, the all-versus-all pairwise alignments were calculated using LAST (70% sequence identity, 80% alignment coverage). The reference genome graph consisted of 71,312,220 nodes (proteins) and 5,313,956,680 edges (pairwise similarities). The graph for the ED proteins consisted of 570,198,677 nodes and 5,196,499,560 edges. Notably, during the similarity matrix construction, 23,359,783 (-24.67%) out of the 94,672,003 reference proteins and 601,776,172 (-51.34%) out of the 1,171,974,849 ED proteins remained as singletons. Using 2,500 compute nodes (170,000 compute cores) of the NERSC Cori supercomputer (Intel KNL partition), HipMCL clustered the reference protein graph in 24 min and the ED protein graph in 3 h and 20 min.

Notably, for this task, we explored several graph- and sequence-based methods such as CD-HIT³⁶, UCLUST³⁷, kClust³⁸ or Louvain³⁹ that could not perform at this scale as well as MMSeq2-linclud⁴⁰ and SPIC⁴¹, which were previously proposed to scale at this data size but none performed sufficiently well for the scope of this work. A comparison among these different clustering strategies is provided in the Supplementary Methods. With regard to sequence identity, we set the cut-off at 70% to achieve a compromise between sensitivity and specificity. Although other resources have used more stringent parameters (such as MGnify⁶, in which sequence clustering is performed with a 90% sequence identity cut-off), focusing on specificity, we have chosen a more sensitivity-based approach, yet not overly sensitive, to avoid artifacts produced by noise, multi-domain effects and false positives. Regarding alignment coverage, the choice of a high-coverage threshold (80%) ensures generating better-quality sequence alignments and avoiding potential artifacts, such as partial hits involving significantly truncated/incomplete genes, pseudogenes and chimeric sequences. The overall quality of the final dataset is further improved by considering MCL clusters with 100 members or more, ensuring the preclusion of spurious gene products. An analysis of how the clustering cut-off values (specifically sequence identity) may influence the quality of the resulting clusters is also provided in the Supplementary Methods.

For each cluster, a multiple-sequence alignment (MSA) was calculated using Clustal Omega⁴². The resulting MSAs were then filtered to

produce seed (non-redundant) alignments using a script written in Python and the ProDy/Evol and Biopython modules⁴³ (90% sequence identity, 75% alignment coverage) (Supplementary Methods). All of the subsequent analysis steps, including the calculation of length distributions, HMM profile training and 3D structure predictions, were performed using the generated seed MSAs. HMM profiles were generated using the hmalign utility of HMMER v.3.1 suite³⁴. The representative consensus sequences for each cluster were calculated with Biopython (Supplementary Methods). Consensus sequences were searched against the whole Pfam-A⁸ database (v.33) HMM profiles with HMMER (inclusion thresholds: 7.0 total, 5.0 domain), as well as against the reference genomes using BLAST⁴⁴ (30% identity, 50% coverage bidirectionally). Initial NMPFs of ≥ 100 members (113,752 clusters from 19,473 datasets with 20,211,137 scaffolds and 21,260,914 proteins) were processed for additional filtering with more stringent criteria to remove sequences with even weak similarities to Pfam-A models or genes from reference genomes, based on their calculated consensus profile sequences. This resulted in a more-stringent set of 106,198 clusters. Clusters of which the consensus sequence was found to have a hit to either Pfam-A or a reference genome were removed. A complete summary of the clustering procedure for each ED dataset is provided in Supplementary Data 3. Plot distributions were computed using R and the R/ggplot2⁴⁵ package. For all calculations regarding NMPF sequence length, the average sequence length of each cluster's seed MSA was calculated and used.

Verification of protein family novelty

Additional searches were performed against the reference proteomes of RefSeq (November 2021 release) using the NMPF clusters' consensus sequences and HMM profiles with LAST (matrix: BLOSUM62, gap open: 11, gap extend: 2) and HMMER (inclusion thresholds: 7.0 total, 5.0 domain), respectively, and applying a 70% alignment coverage cut-off. These searches showed that 5,111 clusters (around 5% of the total) obtained positive hits against 134,273 RefSeq sequences. Taxonomic annotation of these sequences showed that 75,215 (56.01%) of the positive hits were eukaryotic, 46,793 (34.85%) were bacterial, 9,296 (6.92%) were archaeal and 2,905 (2.16%) were viral, with 64 sequences having no taxonomic annotation. About half (70,554 or 52.54%) of the hits were published from 2020 onwards, with the majority of those matching genes from MAGs. Cross-examination of the RefSeq hits with UniProt (release 2021_04) records showed that 31,242 (23.27%) of the RefSeq sequences were mapped to 33,628 UniProtKB entries (453 SwissProt and 33,175 TrEMBL); these sequences correspond to only 32 NMPF clusters. The rest of the RefSeq sequences (103,031) were contained in the UniParc archive of UniProt and had no annotation evidence (either manual or automatically generated). The NMPF clusters were searched against Pfam-B, a non-annotated, computationally generated dataset of alignments for sequences not covered by Pfam-A. This resulted in 8,313 unique clusters with positive hits against 5,310 Pfam-B. Finally, the positive hits against the searches of each dataset were compiled and compared. In total, 12,846 clusters had a positive hit to RefSeq, Pfam-B or both, while the rest of the clusters (93,352) had no hits. Finally, all NMPF sequences were searched against AntiFam⁴⁶ v.6.0, a collection of HMM profiles designed to detect potential spurious protein sequences, pseudogenes and false protein translations. Only 43 sequences were identified, with low-score hits and low alignment coverage (<50%) to two AntiFam profiles.

Ecosystem and taxonomic annotation of protein clusters

NMPF clusters were annotated with available environmental and taxonomy metadata through their associated environmental datasets. In the case of environmental metadata, the GOLD¹⁵ ecosystem classification scheme¹⁴ was used to organize datasets into ecosystem groups (such as freshwater, marine, soil, host-associated); each protein cluster was then assigned to one or more ecosystems on the basis of the ecosystem

information of the ED samples in IMG on which the protein sequences were found. In addition to GOLD, the Environment Ontology (ENVO)⁴⁷ and Earth Microbiome Project Ontology (EMPO)⁴⁸ were considered as potential alternative classification systems. Mapping of ED samples and NMPFs to ENVO and EMPO was performed using the metadata of the GOLD biosample project associated with each ED sample. The ecosystem assignments for all three classification systems are presented in Supplementary Data 5. Ultimately, the GOLD classification was used, as it was found to offer the most diverse options and classified all ED samples and NMPFs. From the 19,326 environmental samples that included the NMPFs, 14,540 (75.24%) were environmental (for example, soil, freshwater), 3,867 (20.01%) were host-associated (for example, human, plants) and 919 (4.76%) came from engineered environments (for example, wastewater, industrial wastes).

In a similar manner, the initial taxonomic annotation for the clusters was performed using the NCBI taxonomy information of the scaffolds contained in each IMG/M dataset, where available. Note that the majority of the scaffolds used in this study were too short and therefore remained unclassified taxonomically. Furthermore, there is very little information on the taxonomy of viral scaffolds. To alleviate these issues, annotations for scaffolds >5 kb that had previously been identified as viral and included in version 3.0 of IMG/VR⁴⁹ were used. Moreover, scaffolds 1–5 kb in length were analysed using DeepVirFinder (v.1.0)⁵⁰, and the generated *P* values were subsequently converted to *q* values using the R package *qvalue*⁵¹ to obtain estimates of the false-discovery rate. Scaffolds with *q* ≤ 0.001 were retained as putative viral scaffolds. Unclassified scaffolds were further analysed using two eukaryotic sequence detection tools, Whokaryote⁵² and EukRep⁵³. Furthermore, the NMPF clusters were searched against the Tara Oceans collection of eukaryotic MAGs⁵⁴. Finally, all remaining unclassified scaffolds were taxonomically assigned using the MMseqs2 taxonomy tool^{40,55}, performing six-frame translation searches against UniRef50⁵⁶ and assigning each analysed scaffold to the lowest common ancestor of the best hits for each frame. The taxonomic assignments of the NMPF clusters were based on the source scaffolds and are given in Supplementary Data 6. A detailed description of the taxonomic annotation and analysis is given in the Supplementary Methods.

Distribution analysis of the protein clusters across ecosystems and NCBI taxa was performed by creating and visualizing networks with Gephi⁵⁷ using the Yifan Hu algorithm⁵⁸ to generate the layout. As the resulting networks, when taking into account all clusters, were very dense, an association threshold was used to filter the data for better clarity, keeping only the edges where at least 2% of the members of each cluster were assigned to a certain ecosystem or phylogeny. Additional analysis was performed by creating circos plots and distribution matrices, produced using the R/chorddiag⁵⁹ and Processing/P5 libraries, respectively. Bar plots were also created in R, using the R/ggplot2⁴⁵ and R/plotly⁶⁰ libraries. Visualizations of geographical distribution were created using maps from the Natural Earth public domain repository (<https://www.naturalearthdata.com/>).

Sequence quality control

The quality of the predicted protein sequences used in the analysis was evaluated by taking into account the predicted gene coordinates and gene density of the source ED scaffolds. In particular, evaluation was performed for scaffolds identified as eukaryotic from the IMG/M pipeline, as well as scaffolds with no taxonomic annotation and low density, as the latter is often indicative of potential eukaryotic contigs, or contigs featuring alternative genetic codes. Furthermore, the distance of each NMPF sequence from its respective scaffold ends was evaluated to detect potentially shortened/truncated genes. Based on the above, a number of metrics have been established to assess the quality of NMPF clusters. Details on the analysis are provided in the Supplementary Methods. The quality assessment of NMPFs is presented in Supplementary Data 7.

Protein cluster co-occurrence with Pfams

The co-occurrence of NMPFs with known protein domains was determined by performing searches for the existence of Pfam protein domains in the analysed scaffolds containing both novel and known protein-coding genes. The translated sequences of the known genes for each scaffold were searched against the HMM profiles of Pfam using HMMER and the HMM profiles' default trusted cut-off. All positive hits were assigned to their respective scaffolds and, in turn, to NMPFs containing novel sequences from these scaffolds, as potential co-occurring domains. The co-occurrence frequency percentage of each Pfam domain for each NMPF was calculated, defined as the number of scaffolds containing this domain over the total number of scaffolds associated with the NMPF. The Pfam domains were subsequently mapped to COG⁷ domains and their functional categories. No associations to Pfam were observed for 7,885 NMPFs; for the rest of the clusters, the top five Pfam and COG hits based on their frequency are reported in Supplementary Data 1. Moreover, the gene neighbourhoods of selected NMPFs were visualized as association networks, built with NORMA (v.2.0)⁶¹, and using COG functional categories to provide annotations.

Protein fold prediction. Multiple-sequence alignment. The query sequence for the MSA was determined by taking the central or pivot sequence of the seed MSA. Query sequences were defined in each MSA by performing pairwise distance calculations, creating an all-against-all distance matrix, and selecting the sequence with the minimum Hamming distance. The MSAs were then recalculated using the central sequence as a guide, filtering to remove sequences poorly aligned to the query (cut-offs set at 90% for sequence identity and 80% for alignment coverage), as well as poorly aligned positions (low column occupancy). The final MSAs were considered for further analysis if they had more than 16 effective sequences. Calculations were performed using Python and the TensorFlow⁶², SciKit⁶³ and Biopython libraries. **TrRosetta for initial screening.** For the initial pass, each of the putative protein families was analysed using TrRosetta²⁵ to obtain a distogram. Notably, a distogram is a tensor that contains the predicted distance distribution for every pair of residues. By summing the distances of less than 8 Å, a distogram can be converted into a contact map, indicating the probability of contact. The mean of the top probabilities has been shown to be highly correlated with structure accuracy²⁶ and can be used to filter for proteins that are probably well structured. This metric is very fast to compute and enables us to quickly scan through 106,198 examples. MSAs with at least 0.5 average probability were selected for AlphaFold prediction, alongside the MSAs with enough effective sequences.

AlphaFold for final prediction. As none of the NMPFs match known protein families (Pfam) or structures in the PDB, AlphaFold²² was run with no template input. Five models were generated per run and the model with the best pLDDT average was selected for downstream evaluation.

Searching for structural homologues. Before any structural search, regions with low predicted confidence (pLDDT < 0.7) were removed. To test whether there is any structural similarity to experimentally determined structures, a TMalign⁶⁴ search was performed against every domain in SCOPe²⁷ (21 October 2021, v.2.0.8), an annotated version of the SCOP⁶⁵ database of protein domains. To test if hits (TM-score > 0.5) were novel assignments (not easily inferred from distant sequence homologues), the TMalign score was also computed for the structure of the top HHsearch hit. Finally, the TM-score could be low owing to the length difference between the target and query. This can happen because the query is multi-domain; to account for this, an additional search was performed against the entire PDB²⁸ (accessed on 17 December 2021) using MMalign⁶⁶. To further confirm that any hits to PDB were non-trivial, we compared the predicted structure to the PDB structure of the top hit from an HMM–HMM alignment search, using HHsearch⁶⁷.

The predicted structures with non-trivial hits to SCOPe that were supported by HHsearch results are referred to as novel assignments.

Clustering. For clustering, the all-versus-all TAlign score was computed for all predicted structures with pTM > 0.7 trimmed to regions with pLDDT > 0.7. Clusters are defined as the connected components of a network, where edges are defined by TM-score > 0.6 for both target-to-query and query-to-target alignment.

Reporting summary

Further information on research design is available in the Nature Portfolio Reporting Summary linked to this article.

Data availability

All of the analysed datasets along with their corresponding sequences are available from the IMG system (<http://img.jgi.doe.gov/>). A list of the datasets used in this study is provided in Supplementary Data 8. All data from the protein clusters, including sequences, multiple alignments, HMM profiles, 3D structure models, and taxonomic and ecosystem annotation, are available through NMPFamsDB, publicly accessible at www.nmpfamsdb.org. The 3D models are also available at ModelArchive under accession code ma-nmpfamsdb.

Code availability

Sequence analysis was performed using Tantan (<https://gitlab.com/mcfrith/tantan>), BLAST (<https://blast.ncbi.nlm.nih.gov/Blast.cgi>), LAST (<https://gitlab.com/mcfrith/last>), HMMER (<http://hmmer.org/>) and HH-suite3 (<https://github.com/soedinglab/hh-suite>). Clustering was performed using HipMCL (<https://bitbucket.org/azadce/hipmcl/src/master/>). Additional taxonomic annotation was performed using Whokaryote (<https://github.com/LottePronk/whokaryote>), EukRep (<https://github.com/patrickwest/EukRep>), DeepVirFinder (<https://github.com/jessieren/DeepVirFinder>) and MMseqs2 (<https://github.com/soedinglab/MMseqs2>). 3D modelling was performed using AlphaFold2 (<https://github.com/deepmind/alphafold>) and TrRosetta2 (<https://github.com/RosettaCommons/trRosetta2>). Structural alignments were performed using TAlign (<https://zhanggroup.org/TM-align/>) and MAlign (<https://zhanggroup.org/MM-align/>). All custom scripts used for the generation and analysis of the data are available at Zenodo (<https://doi.org/10.5281/zenodo.8097349>).

33. Frith, M. C. A new repeat-masking method enables specific detection of homologous sequences. *Nucleic Acids Res.* **39**, e23 (2011).
34. Eddy, S. R. Accelerated Profile HMM Searches. *PLoS Comput. Biol.* **7**, e1002195 (2011).
35. Kietbasa, S. M., Wan, R., Sato, K., Horton, P. & Frith, M. C. Adaptive seeds tame genomic sequence comparison. *Genome Res.* **21**, 487–493 (2011).
36. Li, W. & Godzik, A. Cd-hit: a fast program for clustering and comparing large sets of protein or nucleotide sequences. *Bioinformatics* **22**, 1658–1659 (2006).
37. Edgar, R. C. Search and clustering orders of magnitude faster than BLAST. *Bioinformatics* **26**, 2460–2461 (2010).
38. Hauser, M., Mayer, C. E. & Söding, J. kClust: fast and sensitive clustering of large protein sequence databases. *BMC Bioinform.* **14**, 248 (2013).
39. Blondel, V. D., Guillaume, J.-L., Lambiotte, R. & Lefebvre, E. Fast unfolding of communities in large networks. *J. Stat. Mech.* **2008**, P10008 (2008).
40. Steinegger, M. & Söding, J. MMseqs2 enables sensitive protein sequence searching for the analysis of massive data sets. *Nat. Biotechnol.* **35**, 1026–1028 (2017).
41. Jiang, P. & Singh, M. SPICi: a fast clustering algorithm for large biological networks. *Bioinformatics* **26**, 1105–1111 (2010).
42. Sievers, F. & Higgins, D. G. Clustal Omega for making accurate alignments of many protein sequences. *Protein Sci.* **27**, 135–145 (2018).
43. Cock, P. J. A. et al. Biopython: freely available Python tools for computational molecular biology and bioinformatics. *Bioinformatics* **25**, 1422–1423 (2009).
44. Altschul, S. F., Gish, W., Miller, W., Myers, E. W. & Lipman, D. J. Basic local alignment search tool. *J. Mol. Biol.* **215**, 403–410 (1990).
45. Wickham, H. *ggplot2: Elegant Graphics for Data Analysis* (Springer-Verlag, 2016).
46. Eberhardt, R. Y. et al. AntiFam: a tool to help identify spurious ORFs in protein annotation. *Database* **2012**, bas003 (2012).
47. Buttigieg, P. L. et al. The environment ontology in 2016: bridging domains with increased scope, semantic density, and interoperability. *J. Biomed. Semantics* **7**, 57 (2016).
48. Thompson, L. R. et al. A communal catalogue reveals Earth's multiscale microbial diversity. *Nature* **551**, 457–463 (2017).

49. Roux, S. et al. IMG/VR v3: an integrated ecological and evolutionary framework for interrogating genomes of uncultivated viruses. *Nucleic Acids Res.* **49**, D764–D775 (2021).
50. Ren, J. et al. Identifying viruses from metagenomic data using deep learning. *Quant. Biol.* **8**, 64–77 (2020).
51. Storey, J. D., Bass, A. J., Dabney, A. & Robinson, D. qvalue: Q-value estimation for false discovery rate control. R package version 2.32.0 <http://github.com/jdstorey/qvalue> (2023).
52. Pronk, L. J. U. & Medema, M. H. Whokaryote: distinguishing eukaryotic and prokaryotic contigs in metagenomes based on gene structure. *Microb. Genomics* **8**, mgen000823 (2022).
53. West, P. T., Probst, A. J., Grigoriev, I. V., Thomas, B. C. & Banfield, J. F. Genome-reconstruction for eukaryotes from complex natural microbial communities. *Genome Res.* **28**, 569–580 (2018).
54. Delmont, T. O. et al. Functional repertoire convergence of distantly related eukaryotic plankton lineages abundant in the sunlit ocean. *Cell Genomics* **2**, 100123 (2022).
55. Mirdita, M., Steinegger, M., Breitwieser, F., Söding, J. & Levy Karin, E. Fast and sensitive taxonomic assignment to metagenomic contigs. *Bioinformatics* **37**, 3029–3031 (2021).
56. Suzek, B. E., Wang, Y., Huang, H., McGarvey, P. B. & Wu, C. H. UniRef clusters: a comprehensive and scalable alternative for improving sequence similarity searches. *Bioinformatics* **31**, 926–932 (2015).
57. Bastian, M., Heymann, S. & Jacomy, M. Gephi: an open source software for exploring and manipulating networks. In *Proc. International AAAI Conference on Web and Social Media* Vol. 3, 361–362 (AAAI, 2009).
58. Hu, Y. in *Combinatorial Scientific Computing* (eds Naumann, U. & Schenk, O.) 525–549 (CRC Press, 2010).
59. Flajolet, P. & Noy, M. in *Formal Power Series and Algebraic Combinatorics* (eds Krob, D. et al.) 191–201 (Springer, 2000); https://doi.org/10.1007/978-3-662-04166-6_17.
60. Sievert, C. *Interactive Web-Based Data Visualization with R, plotly, and shiny* (Chapman and Hall/CRC, 2020).
61. Karatzas, E. et al. The network makeup artist (NORMA-2.0): distinguishing annotated groups in a network using innovative layout strategies. *Bioinform. Adv.* **2**, vbac036 (2022).
62. Abadi, M. et al. TensorFlow: large-scale machine learning on heterogeneous systems. Preprint at <https://doi.org/10.48550/arXiv.1603.04467> (2015).
63. Pedregosa, F. et al. Scikit-learn: machine learning in Python. *J. Mach. Learn. Res.* **12**, 2825–2830 (2011).
64. Zhang, Y. & Skolnick, J. TM-align: a protein structure alignment algorithm based on the TM-score. *Nucleic Acids Res.* **33**, 2302–2309 (2005).
65. Andreeva, A., Kulesha, E., Gough, J. & Murzin, A. G. The SCOP database in 2020: expanded classification of representative family and superfamily domains of known protein structures. *Nucleic Acids Res.* **48**, D376–D382 (2020).
66. Mukherjee, S. & Zhang, Y. MM-align: a quick algorithm for aligning multiple-chain protein complex structures using iterative dynamic programming. *Nucleic Acids Res.* **37**, e83 (2009).
67. Steinegger, M. et al. HH-suite3 for fast remote homology detection and deep protein annotation. *BMC Bioinform.* **20**, 473 (2019).

Acknowledgements We thank H. Maughan for reading the paper; and all of the colleagues who contributed to the many facets of metagenomics, from sample collection to sequencing and annotation that made this work possible. The list of the JGI Proposal Award DOIs is available in Supplementary Table 13. This work used resources of the National Energy Research Scientific Computing Center (NERSC), supported by the Office of Science of the US Department of Energy (DOE). Additional computations were performed with the use of the Greek Research and Technology Network (GRNET) Aris High Processing Computing (HPC) infrastructure (project code: PRO09008-BOLOGNA). This work was supported in part by the US DOE Joint Genome Institute (DE-AC02-05CH11231, in part), a DOE Office of Science User Facility; the Applied Mathematics program of the DOE Office of Advanced Scientific Computing Research (DE-AC02-05CH11231, in part), Office of Science of the US DOE; Exascale Computing Project (17-SC-20-SC), a collaborative effort of the US DOE Office of Science and the National Nuclear Security Administration; DOE grant DE-SC0022098. G.A.P., F.A.B. and E.K. were supported by Fondation Santé and the Hellenic Foundation for Research and Innovation (H.F.R.I.) under the 'First Call for H.F.R.I. Research Projects to support faculty members and researchers and the procurement of high-cost research equipment grant' (grant ID HFRI-17-1855-BOLOGNA). G.A.P. also acknowledges the Marie Skłodowska-Curie Individual Fellowships (MSCA-IF-EF-CAR, grant ID 838018, H2020-MSCA-IF-2018) and 'The Greek Research Infrastructure for Personalized Medicine (pMedGR)' (MIS 5002802), which is implemented under the Action 'Reinforcement of the Research and Innovation Infrastructure', funded by the Operational Program 'Competitiveness, Entrepreneurship and Innovation' (NSRF 2014-2020) and co-financed by Greece and the European Union (European Regional Development Fund). C.A.O. and I.I. acknowledge support by the project Elixir-GR (MIS 5002780), implemented under the Action 'Reinforcement of the Research and Innovation Infrastructure', funded by the Operational Program 'Competitiveness, Entrepreneurship and Innovation' (NSRF 2014-2020) and co-financed by Greece and the European Union (European Regional Development Fund). S.O. and S.L. are supported by NIH grant DP5OD026389 and the Moore-Simons Project on the Origin of the Eukaryotic Cell, Simons Foundation 735929LPI (<https://doi.org/10.46714/735929LPI>). J.P.-R. was supported by the US DOE Genomic Sciences Program, award SCW1632; and work conducted at the LLNL was conducted under the auspices of the US DOE under Contract DE-AC52-07NA27344. Work from the consortium was supported by NSF grants OIA-1826734, DEB-1441717 and OCE-1232982; NSF 1921429; CONACYT grants A1-S-9889 and CB-2010-01-151007; US DOE, Office of Science, Office of Biological and Environmental Research (BER), Great Lakes Bioenergy Research Center (DOE BER DE-SC0018409 and DE-FC02-07ER64494); NSF grant OCE-082546, US DOE, Office of Science, Facilities Integrating Collaborations for User Science (FICUS) program, Office of Workforce Development for Teachers and Scientists, Office of Science Graduate Student Research (SCGSR) program; New Zealand Foundation for Research, Science and Technology grant CO1X0306 and National Science Foundation grant 1745341; NSF Division of Chemical,

Article

Bioengineering, Environmental and Transport Systems grants 1438092 and 1643486; NSF OCE-1559179, NSF OCE-1537951, NSF OCE-1459200, Gordon & Betty Moore Foundation Investigator Award 3789; the G. Unger Vetlesen and Ambrose Monell Foundations; the Natural Sciences and Engineering Research Council of Canada; Genome Canada and Genome British Columbia; the PR-INBRE BIRC program (NIH/NIGMS- award number P20 GM103475); Great Lakes Bioenergy Research Center, US DOE, Office of Science, Office of Biological and Environmental Research under award numbers DE-SC0018409 and DE-FC02-07ER64494; the Agriculture and Food Research Initiative, competitive grant 2009-447 35319-05186 from the US Department of Agriculture, National Institute of Food and Agriculture; Sol Leshin Foundation and the Shanbrom Family Fund; Towards Sustainability Foundation, Cornell Sigma Xi, NSERC PGS-D, NSF-BREAD (IOS-0965336), Cornell Biogeochemistry Program, Cornell Crop and Soil Science Department, USDA-NIFA Carbon Cycle (2014-6700322069) and the Cornell Atkinson Center for a Sustainable Future; Office of Science (BER), US DOE (DE-SC0014395); NSF grant OCE 0424602; US DOE, Office of Science, Office of Biological and Environmental Research, Environmental System Science (ESS) Program; Australian Research Council: DP150100244; NSF-OPP 1641019; NSF 1754756; NSF 1442231; NSF award OCE-173723; USDA National Institute of Food and Agriculture Foundational Program (award 2017-67019-26396); USDA NIFA award 2011-67019-30178; BER grant DE-SC0014395; National Science Foundation grant DEB-1927155; US DOE, Office of Science, Office of Biological and Environmental Research, Environmental System Science (ESS) Program; River Corridor Scientific Focus Area (SFA) project at Pacific Northwest National Laboratory (PNNL); grant NNX16AJ62G from NASA Exobiology; NASA Exobiology awards 80NSSC19K1633 and NNX17AK85G; NSF award DEB-1146149; US NSF (DEB 1912525); US DOE Office of Biological and Environmental Research (DE-SC0020382); NSF EAR-1820658; DE-FG02-94ER20137 from the Photosynthetic Systems Program, Division of Chemical Sciences, Geosciences and Biosciences (CSGB), Office of Basic Energy Sciences of the US DOE; Max Planck Society and the BioEnergy Science Center (BESC),

a US DOE Bioenergy Research Center supported by the Office of Biological and Environmental Research in the DOE Office of Science; and US DOE, Office of Science, Biological and Environmental Research, as part of the Plant Microbe Interfaces Scientific Focus Area at Oak Ridge National Laboratory.

Author contributions N.C.K. conceived the project and performed part of the analysis. G.A.P. performed data collection as well as the analysis. F.A.B. assisted in data analysis and implemented the NMPFamsDB database. I.L., N.N.L., A.V. and C.A.O. provided feedback about the strategy and edited parts of the manuscript. E.K. helped with scripting, data analysis and the implementation of the database. A.A., O.S. and A.B. implemented the HipMCL algorithm and ran the clustering. S.O., D.B. and S.L. performed the protein structure predictions and analysis. D.P.-E., A.P.C., S.N. and L.C. helped with the taxonomic classification of scaffolds. J.M.T. and the Metagenome Protein Families Consortium provided data. G.A.P., S.O. and N.C.K. wrote the paper, with feedback from all of the authors. All of the authors read and approved the manuscript.

Competing interests The authors declare no competing interests.

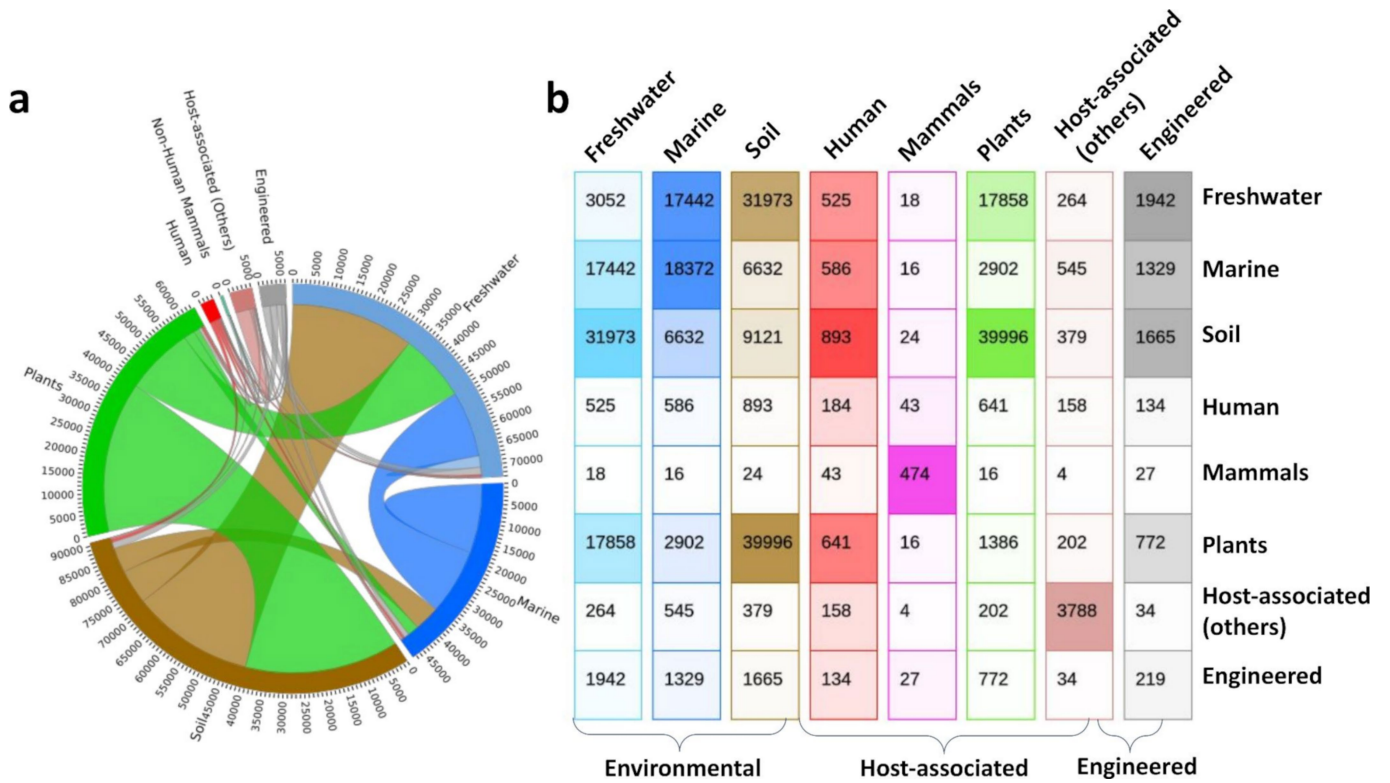
Additional information

Supplementary information The online version contains supplementary material available at <https://doi.org/10.1038/s41586-023-06583-7>.

Correspondence and requests for materials should be addressed to Georgios A. Pavlopoulos or Nikos C. Kyrpides.

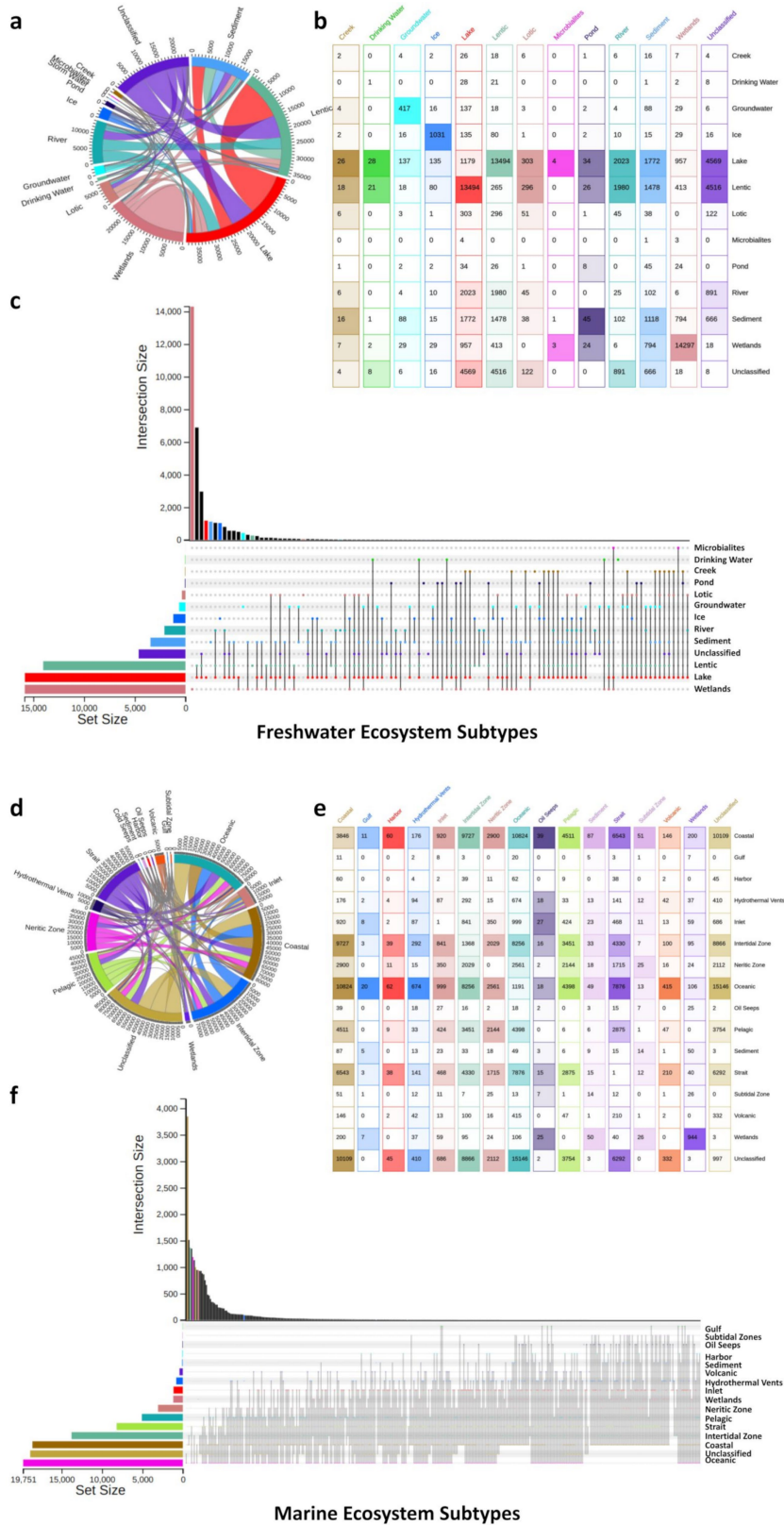
Peer review information *Nature* thanks Ami Bhatt, Alexander Probst and the other, anonymous, reviewer(s) for their contribution to the peer review of this work.

Reprints and permissions information is available at <http://www.nature.com/reprints>.

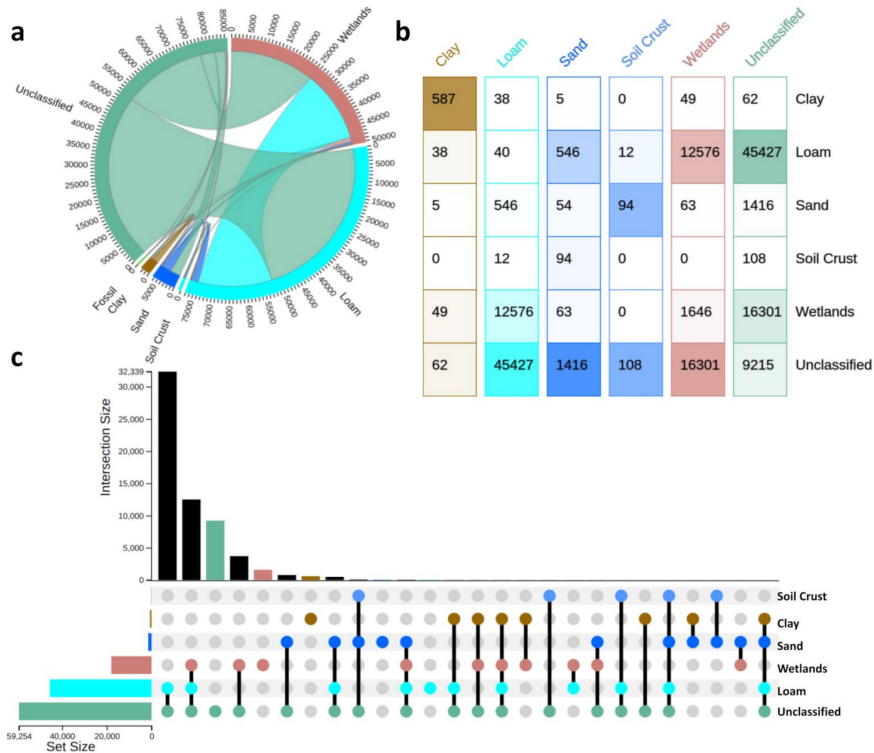


Extended Data Fig. 1 | Distribution of NMPF clusters across the eight ecosystem types. (a) Chord Plot. The distribution of the ecosystems is presented in a chord-like circular diagram. The rim of the diagram represents the total size of the ecosystem types (i.e. number of NMPFs in each ecosystem), with the numbers outside the rim indicating the size scale. The intersections of categories are represented by arcs drawn between them. The size of the arc is proportional to the importance of the flow. (b) 8×8 matrix. Each cell in the

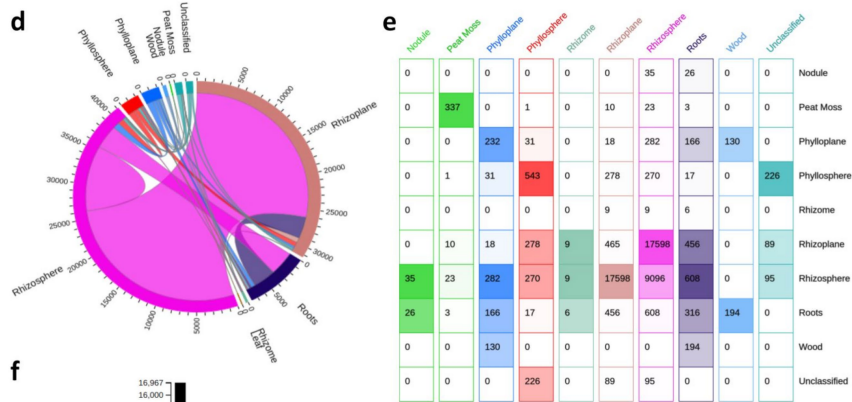
matrix presents the common NMPFs in a binary combination of two ecosystems (e.g. 17,442 NMPFs are common among Marine and Freshwater ecosystems). The diagonal of the matrix displays the ecosystem-specific NMPFs. Each ecosystem column is coloured using the same colour code as Fig. 2, with the brightness of each cell being proportional to the NMPF number (brighter colour = less NMPFs).



Extended Data Fig. 2 | Distribution of NMPF clusters across the sub-categories of the Freshwater (top) and Marine (bottom) aquatic ecosystems. Data are shown as circos plots (a,d), colour-coded matrices (b,e) and UpSet plots (c,f).

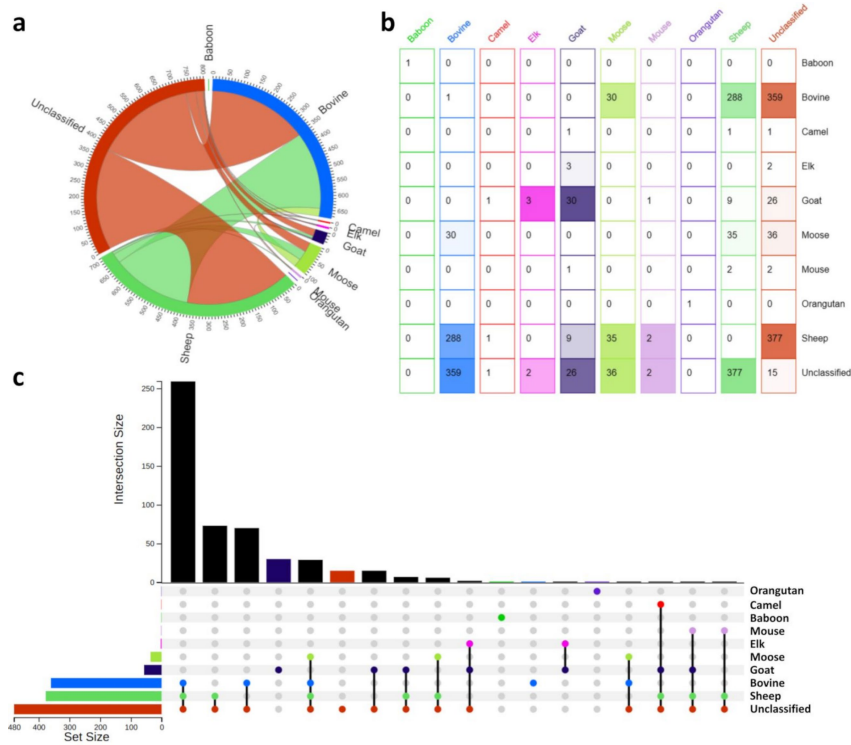


Soil Ecosystem Subtypes

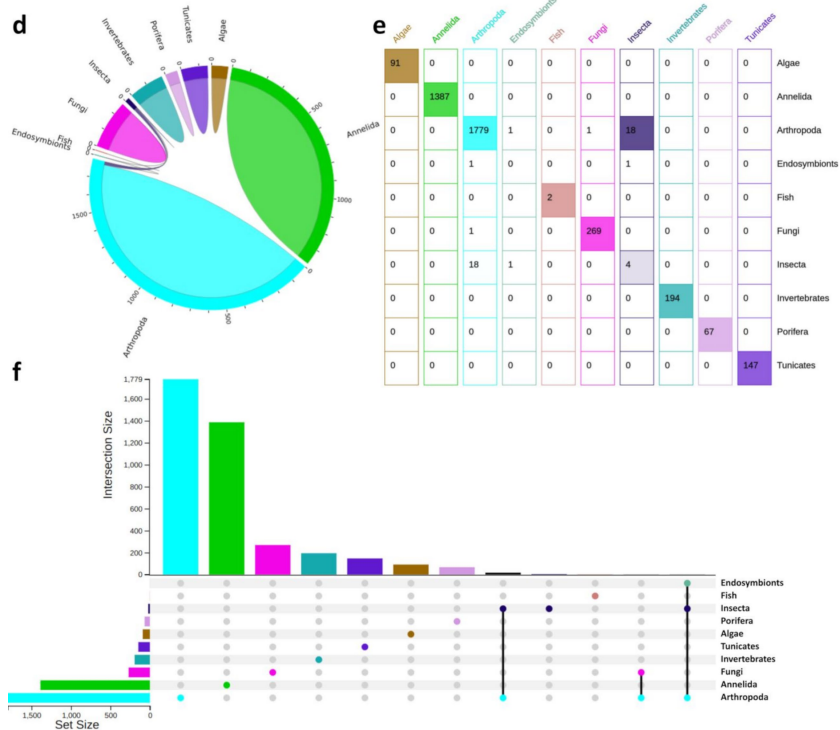


Plant Subtypes

Extended Data Fig. 3 | Distribution of NMPF clusters across the sub-categories of the Soil (top) and Plant (bottom) ecosystems. Data are shown as circo plots (a,d), colour-coded matrices (b,e) and UpSet plots (c,f).

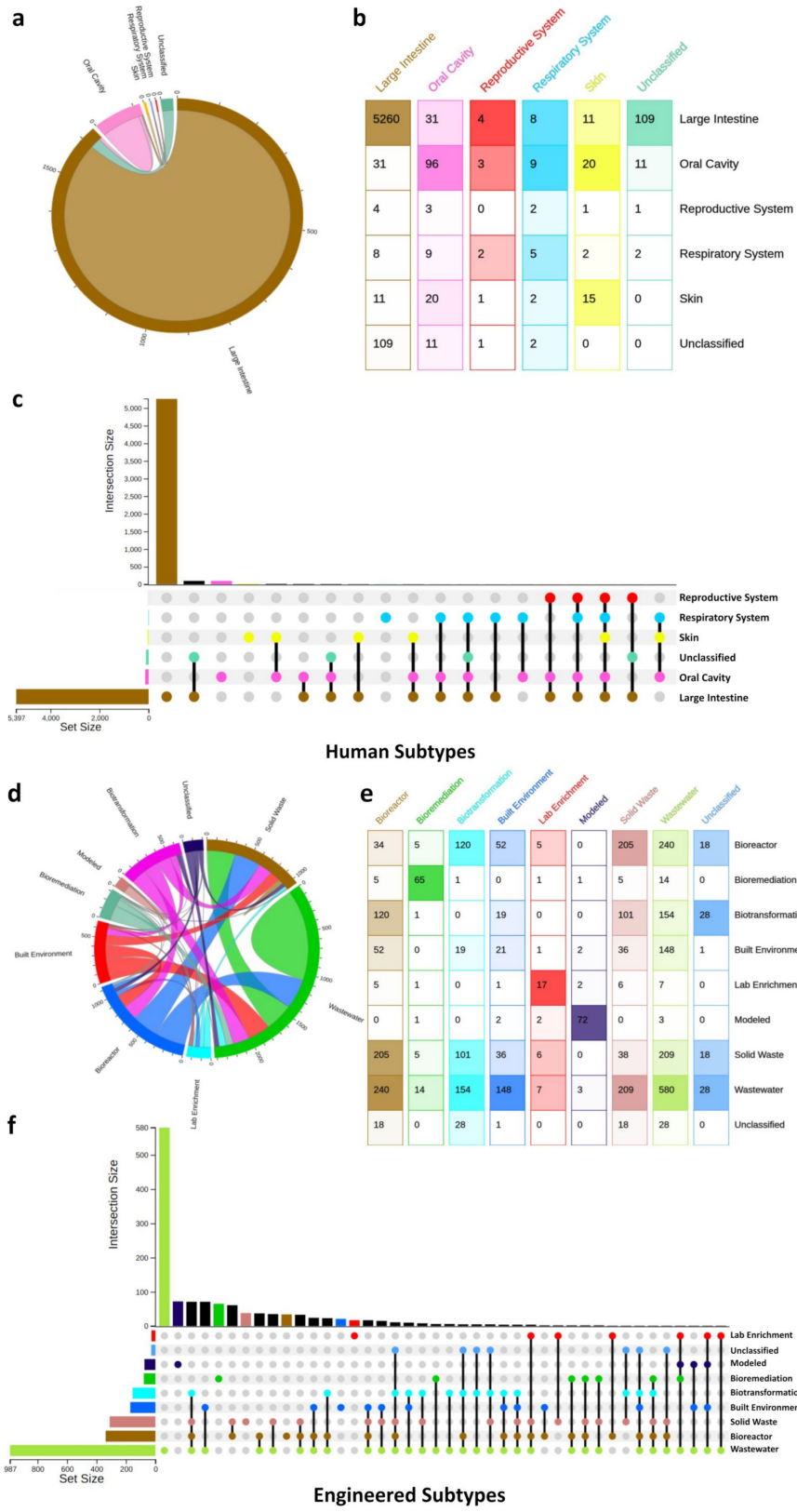


Non-Human Mammal Subtypes



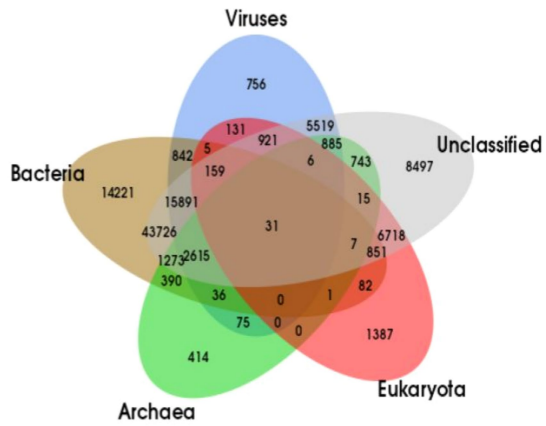
Host-associated (others) Subtypes

Extended Data Fig. 4 | Distribution of NMPF clusters across the sub-categories of the Non-human mammal (top) and Other Host-associated (bottom) ecosystems. Data are shown as circo plots (a,d), colour-coded matrices (b,e) and UpSet plots (c,f).



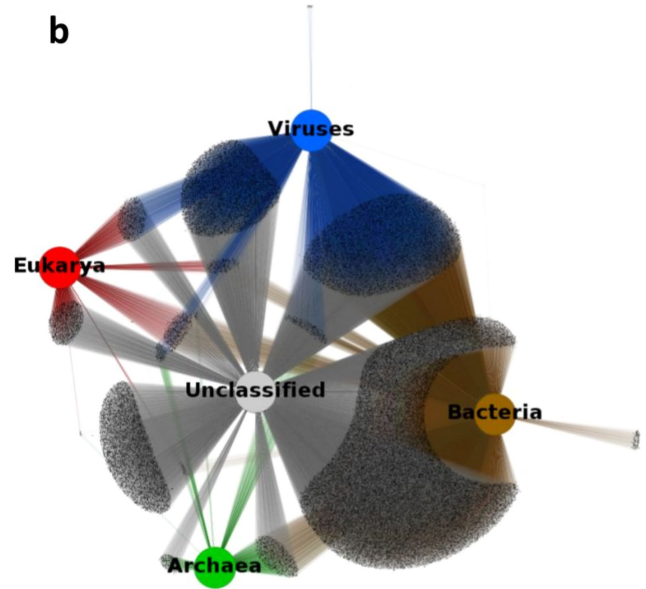
Extended Data Fig. 5 | Distribution of NMPF clusters across the sub-categories of the Human tissue (top) and Engineered (bottom) ecosystems. Data are shown as circos plots (a,d), colour-coded matrices (b,e) and UpSet plots (c,f).

a

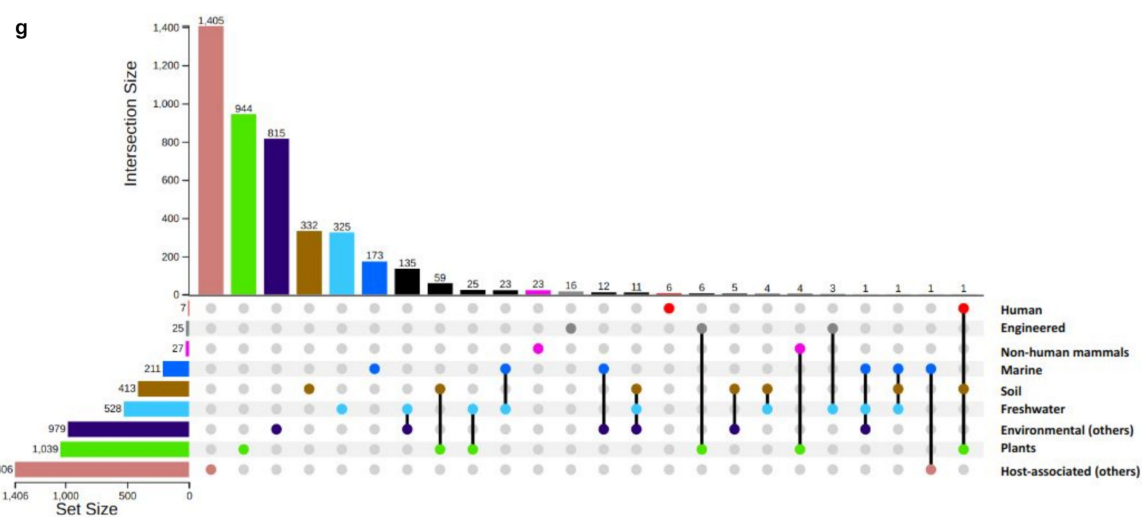
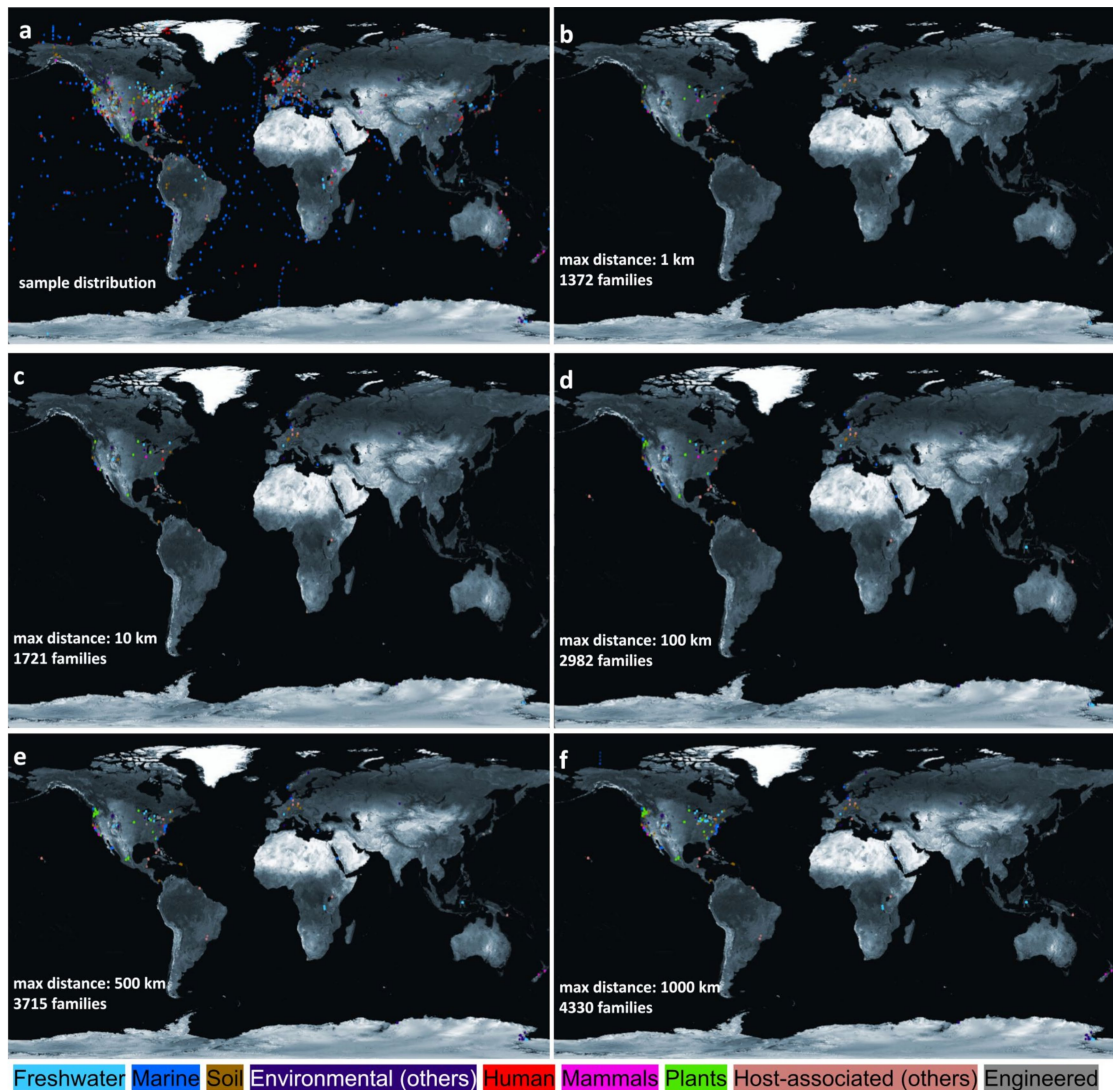


Extended Data Fig. 6 | Distribution of NMPF clusters across different taxa (bacteria, archaea, eukarya, viruses, and unclassified). (a) Venn Diagram, displaying the intersections among the different taxonomy categories.

b

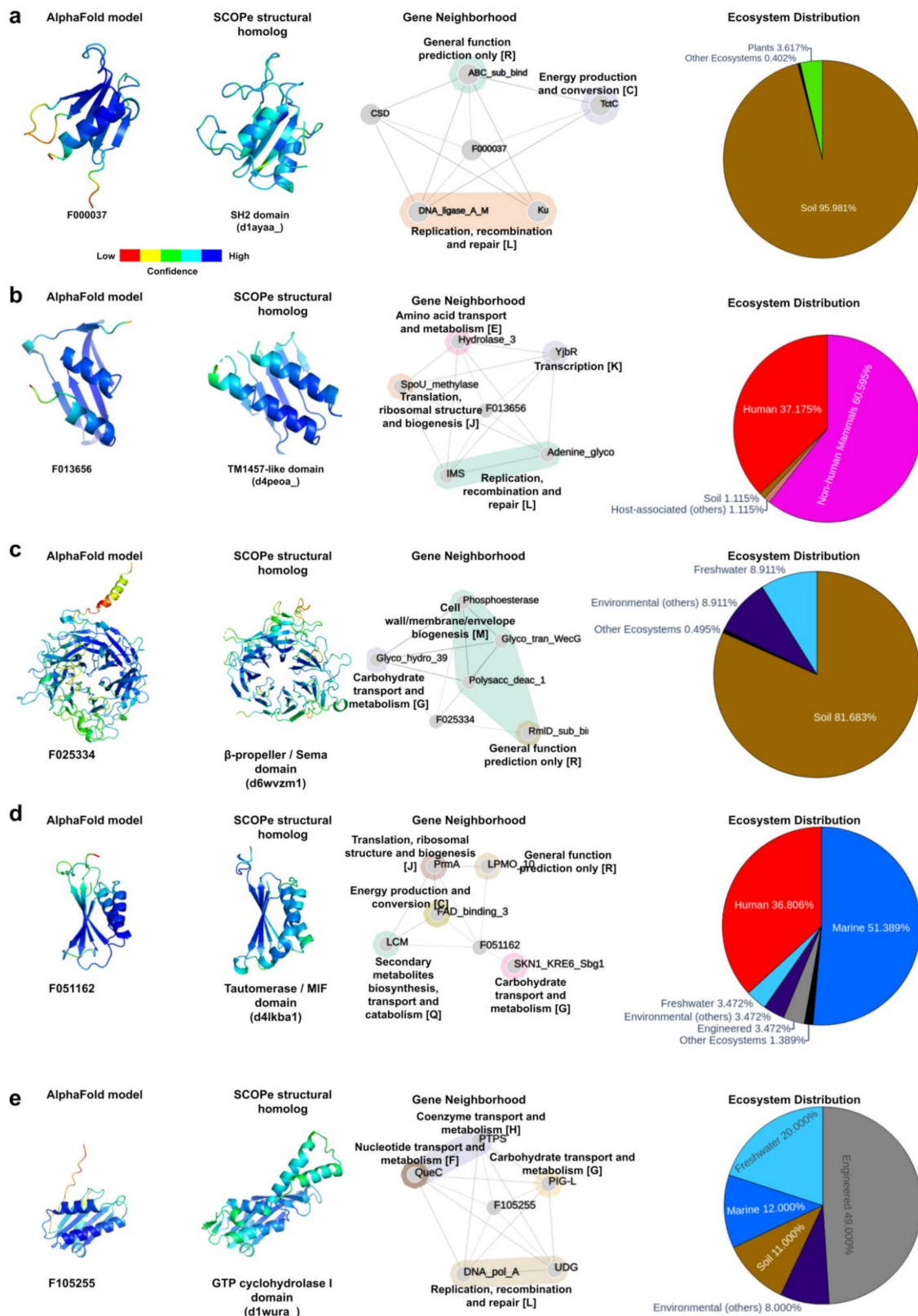


(b) Network representation of the protein clusters and their taxonomic assignments. The taxa are represented by central, coloured nodes (hubs) whereas the grey peripheral nodes represent the protein clusters.



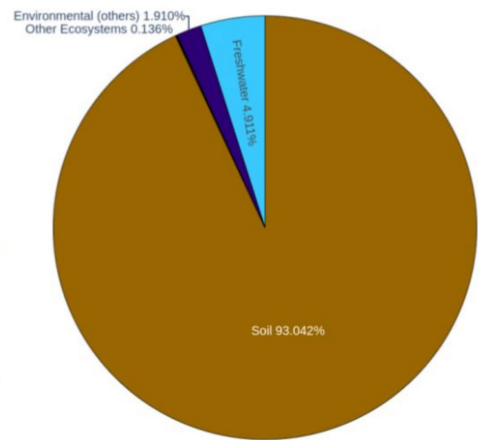
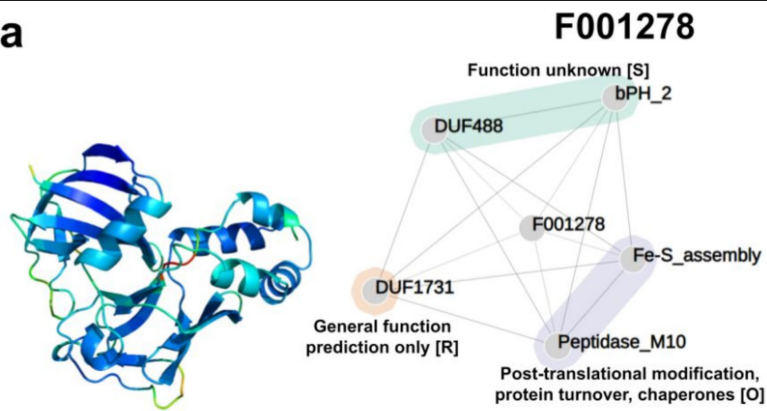
Extended Data Fig. 7 | Geographical distribution of the ED samples and NMPFs. (a) Locations for all ED samples in the study with available geo-location metadata (Longitude and Latitude). (b-f) Distribution of geographically-isolated NMPF clusters, based on a cut-off distance of 1, 10, 100, 500, and 1000 Km. In all cases, dots are coloured based on the ecosystem type (blue: marine, cyan: freshwater, brown: soil, purple: other environmental, green: plants, red: human,

magenta: non-human mammals, salmon pink: other host-associated, grey: engineered). (g) UpSet plot showing the distribution of the geographically-isolated NMPF clusters, based on a cut-off distance of 1000 Km (as shown in panel f). Map panels were created using data from the Natural Earth dataset (www.naturalearthdata.com).



Extended Data Fig. 8 | Functional annotation of NMPFs with remote structural homologues. Five example NMPFs (a-e) are shown. Annotation is performed using structural information (left), gene co-occurrence analysis (middle), and ecosystem distribution (right). Each of the NMPFs has a high-quality 3D model with at least one remote structural homologue to SCOPe. The NMPFs' 3D models, produced with AlphaFold, and the structures of the SCOPe domains are rendered in the same orientation and coloured based on their per-residue structure confidence (pLDDT for AlphaFold models and

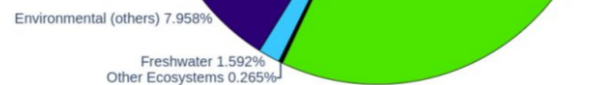
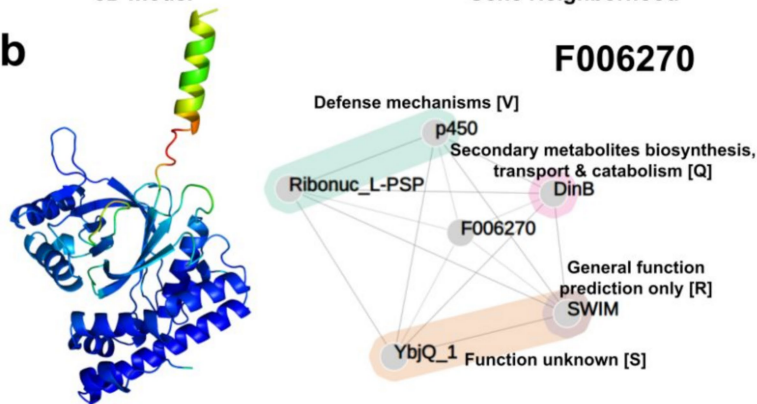
inverse B-factor for experimental structures). The gene neighbourhood of each NMPF is presented in the form of an association network; with nodes representing gene products (the NMPFs and their adjacent genes that encode Pfam domains) and edges representing co-occurrence in the same sequencing scaffold. Pfam domains are further grouped using their associated COG functional categories as annotation. Finally, the NMPFs' associated ecosystems are presented in pie charts. Ecosystems with a <1% presence in the NMPFs are summed into the category "Other ecosystems".

a

3D model

Gene Neighborhood

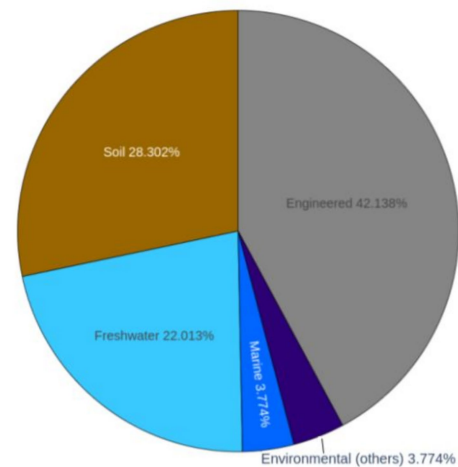
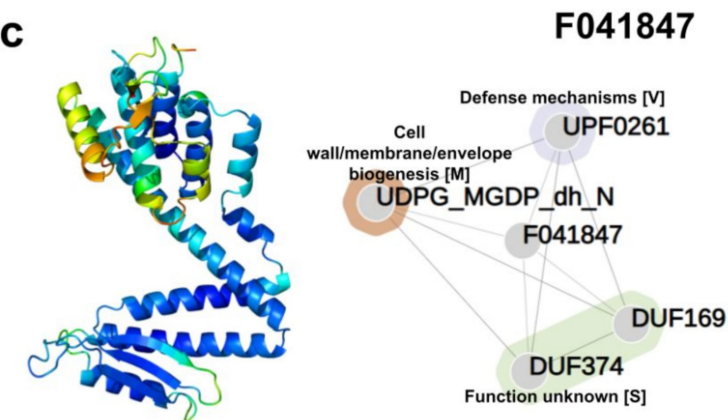
Ecosystem Distribution

b

3D model

Gene Neighborhood

Ecosystem Distribution

c

3D model

Gene Neighborhood

Ecosystem Distribution

Extended Data Fig. 9 | Putative functional annotation of NMPFs with potential novel structural folds. Three example NMPFs (a-c) are shown. The produced AlphaFold 3D model (left), gene co-occurrence analysis (middle) and ecosystem distribution (right) are given. 3D models are coloured based on their per-residue structure confidence (pLDDT). The gene neighbourhood of each NMPF is presented in the form of an association network; with nodes

representing gene products (the NMPFs and their adjacent genes that encode Pfam domains) and edges representing co-occurrence in the same sequencing scaffold. Pfam domains are further grouped using their associated COG functional categories as annotation. Finally, the NMPFs' associated ecosystems are presented in pie charts. Ecosystems with a <1% presence in the NMPFs are summed into the category "Other ecosystems".

Reporting Summary

Nature Portfolio wishes to improve the reproducibility of the work that we publish. This form provides structure for consistency and transparency in reporting. For further information on Nature Portfolio policies, see our [Editorial Policies](#) and the [Editorial Policy Checklist](#).

Statistics

For all statistical analyses, confirm that the following items are present in the figure legend, table legend, main text, or Methods section.

n/a Confirmed

- The exact sample size (n) for each experimental group/condition, given as a discrete number and unit of measurement
- A statement on whether measurements were taken from distinct samples or whether the same sample was measured repeatedly
- The statistical test(s) used AND whether they are one- or two-sided
Only common tests should be described solely by name; describe more complex techniques in the Methods section.
- A description of all covariates tested
- A description of any assumptions or corrections, such as tests of normality and adjustment for multiple comparisons
- A full description of the statistical parameters including central tendency (e.g. means) or other basic estimates (e.g. regression coefficient) AND variation (e.g. standard deviation) or associated estimates of uncertainty (e.g. confidence intervals)
- For null hypothesis testing, the test statistic (e.g. F , t , r) with confidence intervals, effect sizes, degrees of freedom and P value noted
Give P values as exact values whenever suitable.
- For Bayesian analysis, information on the choice of priors and Markov chain Monte Carlo settings
- For hierarchical and complex designs, identification of the appropriate level for tests and full reporting of outcomes
- Estimates of effect sizes (e.g. Cohen's d , Pearson's r), indicating how they were calculated

Our web collection on [statistics for biologists](#) contains articles on many of the points above.

Software and code

Policy information about [availability of computer code](#)

Data collection

Data analysis

For manuscripts utilizing custom algorithms or software that are central to the research but not yet described in published literature, software must be made available to editors and reviewers. We strongly encourage code deposition in a community repository (e.g. GitHub). See the Nature Portfolio [guidelines for submitting code & software](#) for further information.

Data

Policy information about [availability of data](#)

All manuscripts must include a [data availability statement](#). This statement should provide the following information, where applicable:

- Accession codes, unique identifiers, or web links for publicly available datasets
- A description of any restrictions on data availability
- For clinical datasets or third party data, please ensure that the statement adheres to our [policy](#)

All of the analyzed datasets along with their corresponding sequences are available from the IMG system (<http://img.jgi.doe.gov/>). A list of the datasets used in this study is provided as a source data file (IMG_datasets.xlsx) alongside this paper. All data from the protein clusters, including sequences, multiple alignments, HMM profiles, 3D structure models, and taxonomic and ecosystem annotation are available through NMPFamsDB, publicly accessible through www.nmpfamsdb.org. The 3D models are also available in ModelArchive (<https://modelarchive.org>) with the accession code ma-nmpfamsdb through <https://modelarchive.org/doi/10.5452/ma-nmpfamsdb>.

Human research participants

Policy information about [studies involving human research participants and Sex and Gender in Research](#).

Reporting on sex and gender	No human research participants were involved in the study.
Population characteristics	No human research participants were involved in the study.
Recruitment	No human research participants were involved in the study.
Ethics oversight	No human research participants were involved in the study.

Note that full information on the approval of the study protocol must also be provided in the manuscript.

Field-specific reporting

Please select the one below that is the best fit for your research. If you are not sure, read the appropriate sections before making your selection.

- Life sciences Behavioural & social sciences Ecological, evolutionary & environmental sciences

For a reference copy of the document with all sections, see nature.com/documents/nr-reporting-summary-flat.pdf

Life sciences study design

All studies must disclose on these points even when the disclosure is negative.

Sample size	Describe how sample size was determined, detailing any statistical methods used to predetermine sample size OR if no sample-size calculation was performed, describe how sample sizes were chosen and provide a rationale for why these sample sizes are sufficient.
Data exclusions	Describe any data exclusions. If no data were excluded from the analyses, state so OR if data were excluded, describe the exclusions and the rationale behind them, indicating whether exclusion criteria were pre-established.
Replication	Describe the measures taken to verify the reproducibility of the experimental findings. If all attempts at replication were successful, confirm this OR if there are any findings that were not replicated or cannot be reproduced, note this and describe why.
Randomization	Describe how samples/organisms/participants were allocated into experimental groups. If allocation was not random, describe how covariates were controlled OR if this is not relevant to your study, explain why.
Blinding	Describe whether the investigators were blinded to group allocation during data collection and/or analysis. If blinding was not possible, describe why OR explain why blinding was not relevant to your study.

Behavioural & social sciences study design

All studies must disclose on these points even when the disclosure is negative.

Study description	Briefly describe the study type including whether data are quantitative, qualitative, or mixed-methods (e.g. qualitative cross-sectional, quantitative experimental, mixed-methods case study).
-------------------	---

Research sample	State the research sample (e.g. Harvard university undergraduates, villagers in rural India) and provide relevant demographic information (e.g. age, sex) and indicate whether the sample is representative. Provide a rationale for the study sample chosen. For studies involving existing datasets, please describe the dataset and source.
Sampling strategy	Describe the sampling procedure (e.g. random, snowball, stratified, convenience). Describe the statistical methods that were used to predetermine sample size OR if no sample-size calculation was performed, describe how sample sizes were chosen and provide a rationale for why these sample sizes are sufficient. For qualitative data, please indicate whether data saturation was considered, and what criteria were used to decide that no further sampling was needed.
Data collection	Provide details about the data collection procedure, including the instruments or devices used to record the data (e.g. pen and paper, computer, eye tracker, video or audio equipment) whether anyone was present besides the participant(s) and the researcher, and whether the researcher was blind to experimental condition and/or the study hypothesis during data collection.
Timing	Indicate the start and stop dates of data collection. If there is a gap between collection periods, state the dates for each sample cohort.
Data exclusions	If no data were excluded from the analyses, state so OR if data were excluded, provide the exact number of exclusions and the rationale behind them, indicating whether exclusion criteria were pre-established.
Non-participation	State how many participants dropped out/declined participation and the reason(s) given OR provide response rate OR state that no participants dropped out/declined participation.
Randomization	If participants were not allocated into experimental groups, state so OR describe how participants were allocated to groups, and if allocation was not random, describe how covariates were controlled.

Ecological, evolutionary & environmental sciences study design

All studies must disclose on these points even when the disclosure is negative.

Study description	We have developed a computational approach to generate reference-free protein families from the sequence space in metagenomes. We have analyzed 26,931 metagenomes and identified 1.17 billion protein sequences longer than 35 amino acids with no similarity to any sequences from 102,491 reference genomes or Pfam. Using massively parallel graph-based clustering, we grouped these proteins into 106,198 novel sequence clusters with more than 100 members, more than doubling the number of protein families obtained from the reference genomes clustered using the same approach. We have annotated these families based on their taxonomic, habitat, geographic and gene neighborhood distributions and, where sufficient sequence diversity was available, predicted protein structures using AlphaFold, revealing novel structures.
Research sample	The research sample consisted of a collection of 8,364,611,943 predicted protein sequences from 26,931 publicly available metagenome and metatranscriptome datasets in IMG/M, as well as a collection of 94,672,003 from all isolate genomes in IMG/M (reference dataset). For each metagenome or metatranscriptome dataset, the analyzed data included the sequencing scaffolds and their predicted gene products, the associated ecosystem and phylogenetic metadata.
Sampling strategy	No statistical-based sample size calculation was performed. The datasets consisted of all publicly available data in IMG/M.
Data collection	Data collection involved retrieving and analyzing sequences from IMG/M. Additional data was retrieved from reference databases to compare, analyze and annotate our results (e.g. Pfam, NCBI RefSeq etc).
Timing and spatial scale	Datasets were collected from the July 2019 release of IMG/M.
Data exclusions	The study focused on publicly available IMG/M datasets. Private datasets were not considered, as they have not yet been released to the public.
Reproducibility	No experimental trials were performed. All data analysis is described in detail in the Methods section of the manuscript.
Randomization	Randomization was not a relevant feature, as work involved computational analysis of metagenome datasets and had no experiments involving samples, organisms or participants.
Blinding	Blinding was not a relevant feature, as the study focuses on the computational analysis of data. In addition, each analysis was performed by multiple participants for validation.

Did the study involve field work? Yes No

Field work, collection and transport

Field conditions	Describe the study conditions for field work, providing relevant parameters (e.g. temperature, rainfall).
------------------	---

Location	<i>State the location of the sampling or experiment, providing relevant parameters (e.g. latitude and longitude, elevation, water depth).</i>
Access & import/export	<i>Describe the efforts you have made to access habitats and to collect and import/export your samples in a responsible manner and in compliance with local, national and international laws, noting any permits that were obtained (give the name of the issuing authority, the date of issue, and any identifying information).</i>
Disturbance	<i>Describe any disturbance caused by the study and how it was minimized.</i>

Reporting for specific materials, systems and methods

We require information from authors about some types of materials, experimental systems and methods used in many studies. Here, indicate whether each material, system or method listed is relevant to your study. If you are not sure if a list item applies to your research, read the appropriate section before selecting a response.

Materials & experimental systems

n/a	Involved in the study
<input checked="" type="checkbox"/>	<input type="checkbox"/> Antibodies
<input checked="" type="checkbox"/>	<input type="checkbox"/> Eukaryotic cell lines
<input checked="" type="checkbox"/>	<input type="checkbox"/> Palaeontology and archaeology
<input checked="" type="checkbox"/>	<input type="checkbox"/> Animals and other organisms
<input checked="" type="checkbox"/>	<input type="checkbox"/> Clinical data
<input checked="" type="checkbox"/>	<input type="checkbox"/> Dual use research of concern

Methods

n/a	Involved in the study
<input checked="" type="checkbox"/>	<input type="checkbox"/> ChIP-seq
<input checked="" type="checkbox"/>	<input type="checkbox"/> Flow cytometry
<input checked="" type="checkbox"/>	<input type="checkbox"/> MRI-based neuroimaging

Antibodies

Antibodies used	<i>Describe all antibodies used in the study; as applicable, provide supplier name, catalog number, clone name, and lot number.</i>
Validation	<i>Describe the validation of each primary antibody for the species and application, noting any validation statements on the manufacturer's website, relevant citations, antibody profiles in online databases, or data provided in the manuscript.</i>

Eukaryotic cell lines

Policy information about [cell lines and Sex and Gender in Research](#)

Cell line source(s)	<i>State the source of each cell line used and the sex of all primary cell lines and cells derived from human participants or vertebrate models.</i>
Authentication	<i>Describe the authentication procedures for each cell line used OR declare that none of the cell lines used were authenticated.</i>
Mycoplasma contamination	<i>Confirm that all cell lines tested negative for mycoplasma contamination OR describe the results of the testing for mycoplasma contamination OR declare that the cell lines were not tested for mycoplasma contamination.</i>
Commonly misidentified lines (See ICLAC register)	<i>Name any commonly misidentified cell lines used in the study and provide a rationale for their use.</i>

Palaeontology and Archaeology

Specimen provenance	<i>Provide provenance information for specimens and describe permits that were obtained for the work (including the name of the issuing authority, the date of issue, and any identifying information). Permits should encompass collection and, where applicable, export.</i>
Specimen deposition	<i>Indicate where the specimens have been deposited to permit free access by other researchers.</i>
Dating methods	<i>If new dates are provided, describe how they were obtained (e.g. collection, storage, sample pretreatment and measurement), where they were obtained (i.e. lab name), the calibration program and the protocol for quality assurance OR state that no new dates are provided.</i>
<input type="checkbox"/>	Tick this box to confirm that the raw and calibrated dates are available in the paper or in Supplementary Information.
Ethics oversight	<i>Identify the organization(s) that approved or provided guidance on the study protocol, OR state that no ethical approval or guidance was required and explain why not.</i>

Note that full information on the approval of the study protocol must also be provided in the manuscript.

Animals and other research organisms

Policy information about [studies involving animals](#); [ARRIVE guidelines](#) recommended for reporting animal research, and [Sex and Gender in Research](#)

Laboratory animals	<i>For laboratory animals, report species, strain and age OR state that the study did not involve laboratory animals.</i>
Wild animals	<i>Provide details on animals observed in or captured in the field; report species and age where possible. Describe how animals were caught and transported and what happened to captive animals after the study (if killed, explain why and describe method; if released, say where and when) OR state that the study did not involve wild animals.</i>
Reporting on sex	<i>Indicate if findings apply to only one sex; describe whether sex was considered in study design, methods used for assigning sex. Provide data disaggregated for sex where this information has been collected in the source data as appropriate; provide overall numbers in this Reporting Summary. Please state if this information has not been collected. Report sex-based analyses where performed, justify reasons for lack of sex-based analysis.</i>
Field-collected samples	<i>For laboratory work with field-collected samples, describe all relevant parameters such as housing, maintenance, temperature, photoperiod and end-of-experiment protocol OR state that the study did not involve samples collected from the field.</i>
Ethics oversight	<i>Identify the organization(s) that approved or provided guidance on the study protocol, OR state that no ethical approval or guidance was required and explain why not.</i>

Note that full information on the approval of the study protocol must also be provided in the manuscript.

Clinical data

Policy information about [clinical studies](#)

All manuscripts should comply with the ICMJE [guidelines for publication of clinical research](#) and a completed [CONSORT checklist](#) must be included with all submissions.

Clinical trial registration	<i>Provide the trial registration number from ClinicalTrials.gov or an equivalent agency.</i>
Study protocol	<i>Note where the full trial protocol can be accessed OR if not available, explain why.</i>
Data collection	<i>Describe the settings and locales of data collection, noting the time periods of recruitment and data collection.</i>
Outcomes	<i>Describe how you pre-defined primary and secondary outcome measures and how you assessed these measures.</i>

Dual use research of concern

Policy information about [dual use research of concern](#)

Hazards

Could the accidental, deliberate or reckless misuse of agents or technologies generated in the work, or the application of information presented in the manuscript, pose a threat to:

No	Yes	
<input type="checkbox"/>	<input type="checkbox"/>	Public health
<input type="checkbox"/>	<input type="checkbox"/>	National security
<input type="checkbox"/>	<input type="checkbox"/>	Crops and/or livestock
<input type="checkbox"/>	<input type="checkbox"/>	Ecosystems
<input type="checkbox"/>	<input type="checkbox"/>	Any other significant area

Experiments of concern

Does the work involve any of these experiments of concern:

- | No | Yes | |
|--------------------------|--------------------------|---|
| <input type="checkbox"/> | <input type="checkbox"/> | Demonstrate how to render a vaccine ineffective |
| <input type="checkbox"/> | <input type="checkbox"/> | Confer resistance to therapeutically useful antibiotics or antiviral agents |
| <input type="checkbox"/> | <input type="checkbox"/> | Enhance the virulence of a pathogen or render a nonpathogen virulent |
| <input type="checkbox"/> | <input type="checkbox"/> | Increase transmissibility of a pathogen |
| <input type="checkbox"/> | <input type="checkbox"/> | Alter the host range of a pathogen |
| <input type="checkbox"/> | <input type="checkbox"/> | Enable evasion of diagnostic/detection modalities |
| <input type="checkbox"/> | <input type="checkbox"/> | Enable the weaponization of a biological agent or toxin |
| <input type="checkbox"/> | <input type="checkbox"/> | Any other potentially harmful combination of experiments and agents |

ChIP-seq

Data deposition

- Confirm that both raw and final processed data have been deposited in a public database such as [GEO](#).
- Confirm that you have deposited or provided access to graph files (e.g. BED files) for the called peaks.

Data access links

May remain private before publication.

For "Initial submission" or "Revised version" documents, provide reviewer access links. For your "Final submission" document, provide a link to the deposited data.

Files in database submission

Provide a list of all files available in the database submission.

Genome browser session

(e.g. [UCSC](#))

Provide a link to an anonymized genome browser session for "Initial submission" and "Revised version" documents only, to enable peer review. Write "no longer applicable" for "Final submission" documents.

Methodology

Replicates

Describe the experimental replicates, specifying number, type and replicate agreement.

Sequencing depth

Describe the sequencing depth for each experiment, providing the total number of reads, uniquely mapped reads, length of reads and whether they were paired- or single-end.

Antibodies

Describe the antibodies used for the ChIP-seq experiments; as applicable, provide supplier name, catalog number, clone name, and lot number.

Peak calling parameters

Specify the command line program and parameters used for read mapping and peak calling, including the ChIP, control and index files used.

Data quality

Describe the methods used to ensure data quality in full detail, including how many peaks are at FDR 5% and above 5-fold enrichment.

Software

Describe the software used to collect and analyze the ChIP-seq data. For custom code that has been deposited into a community repository, provide accession details.

Flow Cytometry

Plots

Confirm that:

- The axis labels state the marker and fluorochrome used (e.g. CD4-FITC).
- The axis scales are clearly visible. Include numbers along axes only for bottom left plot of group (a 'group' is an analysis of identical markers).
- All plots are contour plots with outliers or pseudocolor plots.
- A numerical value for number of cells or percentage (with statistics) is provided.

Methodology

Sample preparation

Describe the sample preparation, detailing the biological source of the cells and any tissue processing steps used.

Instrument

Identify the instrument used for data collection, specifying make and model number.

- Software *Describe the software used to collect and analyze the flow cytometry data. For custom code that has been deposited into a community repository, provide accession details.*
- Cell population abundance *Describe the abundance of the relevant cell populations within post-sort fractions, providing details on the purity of the samples and how it was determined.*
- Gating strategy *Describe the gating strategy used for all relevant experiments, specifying the preliminary FSC/SSC gates of the starting cell population, indicating where boundaries between "positive" and "negative" staining cell populations are defined.*
- Tick this box to confirm that a figure exemplifying the gating strategy is provided in the Supplementary Information.

Magnetic resonance imaging

Experimental design

- Design type *Indicate task or resting state; event-related or block design.*
- Design specifications *Specify the number of blocks, trials or experimental units per session and/or subject, and specify the length of each trial or block (if trials are blocked) and interval between trials.*
- Behavioral performance measures *State number and/or type of variables recorded (e.g. correct button press, response time) and what statistics were used to establish that the subjects were performing the task as expected (e.g. mean, range, and/or standard deviation across subjects).*

Acquisition

- Imaging type(s) *Specify: functional, structural, diffusion, perfusion.*
- Field strength *Specify in Tesla*
- Sequence & imaging parameters *Specify the pulse sequence type (gradient echo, spin echo, etc.), imaging type (EPI, spiral, etc.), field of view, matrix size, slice thickness, orientation and TE/TR/flip angle.*
- Area of acquisition *State whether a whole brain scan was used OR define the area of acquisition, describing how the region was determined.*
- Diffusion MRI Used Not used

Preprocessing

- Preprocessing software *Provide detail on software version and revision number and on specific parameters (model/functions, brain extraction, segmentation, smoothing kernel size, etc.).*
- Normalization *If data were normalized/standardized, describe the approach(es): specify linear or non-linear and define image types used for transformation OR indicate that data were not normalized and explain rationale for lack of normalization.*
- Normalization template *Describe the template used for normalization/transformation, specifying subject space or group standardized space (e.g. original Talairach, MNI305, ICBM152) OR indicate that the data were not normalized.*
- Noise and artifact removal *Describe your procedure(s) for artifact and structured noise removal, specifying motion parameters, tissue signals and physiological signals (heart rate, respiration).*
- Volume censoring *Define your software and/or method and criteria for volume censoring, and state the extent of such censoring.*

Statistical modeling & inference

- Model type and settings *Specify type (mass univariate, multivariate, RSA, predictive, etc.) and describe essential details of the model at the first and second levels (e.g. fixed, random or mixed effects; drift or auto-correlation).*
- Effect(s) tested *Define precise effect in terms of the task or stimulus conditions instead of psychological concepts and indicate whether ANOVA or factorial designs were used.*
- Specify type of analysis: Whole brain ROI-based Both
- Statistic type for inference (See [Eklund et al. 2016](#)) *Specify voxel-wise or cluster-wise and report all relevant parameters for cluster-wise methods.*
- Correction *Describe the type of correction and how it is obtained for multiple comparisons (e.g. FWE, FDR, permutation or Monte Carlo).*

Models & analysis

- n/a | Involved in the study
- Functional and/or effective connectivity
- Graph analysis
- Multivariate modeling or predictive analysis

Functional and/or effective connectivity

Report the measures of dependence used and the model details (e.g. Pearson correlation, partial correlation, mutual information).

Graph analysis

Report the dependent variable and connectivity measure, specifying weighted graph or binarized graph, subject- or group-level, and the global and/or node summaries used (e.g. clustering coefficient, efficiency, etc.).

Multivariate modeling and predictive analysis

Specify independent variables, features extraction and dimension reduction, model, training and evaluation metrics.